ORNL/TM-2018/1040

Summary Report on Effects of Irradiation on Material IG-110 - Prepared for Toyo Tanso Co., Ltd.

Anne A. Campbell
Yutai Katoh

November 2018

OAK RIDGE NATIONAL LABORATORY
MANAGED BY UT-BATTELLE FOR THE US DEPARTMENT OF ENERGY

ORNL/TM-2018/1040

Irradiation effects study of Toyo Tanso HTGR Graphite, Part II: Irradiation and Post-irradiation examination
DOE Project No. NFE-10-02974

SUMMARY REPORT ON EFFECTS OF IRRADIATION ON MATERIAL IG-110 - PREPARED FOR TOYO TANSO CO., LTD.

Anne A. Campbell
Yutai Katoh

Date Published: November 2018

Prepared by
OAK RIDGE NATIONAL LABORATORY
Oak Ridge, Tennessee 37831-6283
managed by
UT-BATTELLE, LLC
for the
US DEPARTMENT OF ENERGY
under contract DE-AC05-00OR22725

CONTENTS

Page

LIST OF FIGURES

Figure **Page**

LIST OF TABLES

Table **Page**

ACRONYMS

AG	Against Gravity
ASME	American Society of Mechanical Engineers
ASTM	American Society for Testing and Materials
AX	Axial
CTE	Coefficient of Thermal Expansion
DOE	Department of Energy
HFIR	High Flux Isotope Reactor
HTGR	High Temperature Gas-cooled nuclear Reactor
LAMDA	Low Activation Materials Development and Analysis
ORNL	Oak Ridge National Laboratory
PSSV	Pre-Irradiation Specimen Size Validation
RSS	Research Safety Summary
SBMS	Standard Based Management System
SiC	Silicon Carbide
TR	Transverse
WG	With Gravity

EXECUTIVE SUMMARY

This joint program between Oak Ridge National Laboratory (ORNL) and Toyo Tanso Co., Ltd., began in 2010 with the final objective being the creation of qualification data of graphite grade IG-110 as a candidate material for use in the Generation-IV high temperature gas-cooled nuclear reactor (HTGR). The first segment of this program involved the planning and design of the irradiation program, and the investigation of the feasibility of using specimens smaller than recommended in the pertinent American Society for Testing and Materials (ASTM) International test standards. The results from the first segment were provided to the program sponsor in the document titled "Graphite Pre-Irradiation Specimen Size Validation and Testing Program - Results - Toyo Tanso Japan" [1]. The second segment of this program included the irradiation of the graphite and the measurement of the changes to a set of pre-defined physical, mechanical, and thermal properties. The third segment of this program studies the irradiation-induced creep due to an applied compression stress.

This report contains the information regarding the planning, implementation of, and the results from the second and third segments of this program. The irradiation program was designed to cover a range of temperature and fluences that are relevant to the conditions expected to occur over the lifetime of the HTGR. The specimens were irradiated in irradiation capsules (called rabbits) in the High Flux Isotope Reactor (HFIR) at ORNL. The post-irradiation property measurements were performed in the Low Activation Materials Design and Analysis (LAMDA) laboratory. The changes in the various properties will be summarized, followed by a discussion on the comparison of the observed changes and similarity to changes in other nuclear graphite grades.

The properties measured, before and after neutron irradiation, include: mass, dimension, Young's modulus (impulse excitation), 4-point flexural strength, compression strength, coefficient of thermal expansion (CTE), and thermal diffusivity/conductivity. This work also included three irradiation creep experiments. The trends observed in these property changes agree well with those reported in the literature for other graphite grades.

The results of the irradiation-induced changes to materials properties, and preliminary creep results were previously published [2]. The data from the previous report is included in this document. All results from this report supersede the results reported previously.

ACKNOWLEDGEMENT

This program would not have been completed without the expertise and input from numerous persons throughout the laboratory. Special notice needs to be given to the staff of the LAMDA laboratory: Joshua Schmidlin, Patricia Tedder, Stephanie Curlin, Michael McAllister, Bill Comings, Brian Eckhart, J. Felipe Mora, and Wallace Porter.

Research sponsored by Toyo Tanso Co., Ltd. under contract NFE-10-02974 with UT-Battelle, LLC. A portion of this research at ORNL's High Flux Isotope Reactor was sponsored by the Scientific User Facilities Division, Office of Basic Energy Sciences, U.S. Department of Energy. Oak Ridge National Laboratory is managed by UT-Battelle, LLC under Contract No. DE-AC05-00OR22725 for the U.S. Department of Energy.

1. INTRODUCTION

This report summarizes the results from the joint research venture, between Oak Ridge National Laboratory (ORNL) and Toyo Tanso Co., Ltd., to study the effect of neutron irradiation on a nuclear graphite grade IG-110. The irradiations were performed in the flux trap of the ORNL High Flux Isotope Reactor (HFIR). This report will cover the basics of the program (material, properties, and irradiation) and the results of the various property changes due to different irradiation conditions (temperature and total fluence). The properties under investigation include: mass, dimension, Young's modulus, 4-point flexural strength, compression strength, coefficient of thermal expansion (CTE), thermal diffusivity/conductivity, and irradiation creep.

The results of the irradiation-induced changes to materials properties, and preliminary creep results were previously published [2]. The data from the previous report is included in this document. All results from this report supersede the results reported previously.

2. MATERIALS

2.1 MATERIALS USED IN THIS PROGRAM

The material of interest was Toyo Tanso Co., Ltd. Grade IG-110, provided by the program sponsor. In extruded and pressed graphite, two orientation indications were used to distinguish the directions of preferred orientation. These directions were usually labeled With Grain and Against Grain. But, in near-isotropic graphite this distinction is difficult to make, and instead the two labels that were used are With Gravity (WG) and Against Gravity (AG), where the WG direction is parallel to the direction of gravity during the isostatic pressing portion of the manufacture process. These distinctions can easily be confused so another way of labeling these directions in isostatically pressed graphite is the use of Axial (AX) and Transverse (TR) indicators, where axial and with gravity indicate the same direction. A schematic representation of the different directions is given in Figure 2.1. The use of AX and TR to define these directions was used throughout this program.

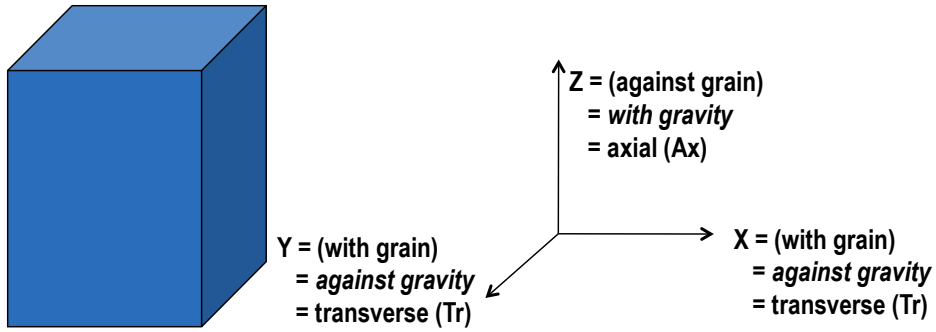

Figure 2.1. Orientation of orthogonal directions, relative to billet molding directions.

2.2 SPECIMEN INFORMATION

Specimens were cut from the larger material blocks. Various specimen sizes and shapes were employed to investigate different physical, thermal, and mechanical properties. Additionally, some specimens were cut with multiple orientations relative to the bulk material to investigate pre-irradiation anisotropy and if there were any effects of orientation on the irradiation behavior. Figure 2.2 shows the different specimen shapes, sizes, and orientations, relative to the orthogonal directions of the bulk material. A summary of these specimen types, dimensions, and uses are in Table 2.1.

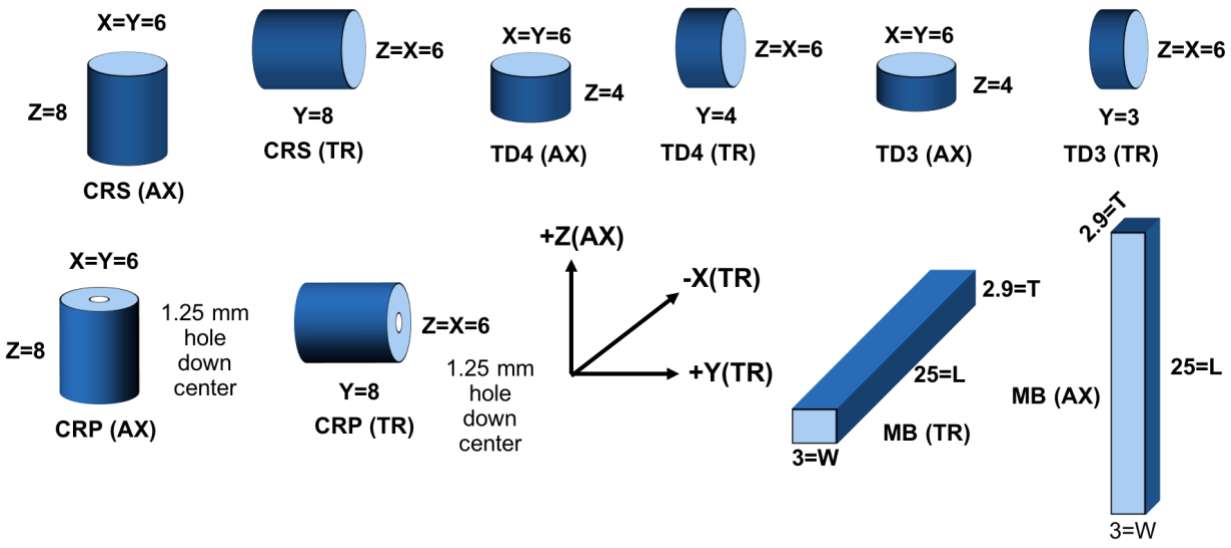

Figure 2.2. Specimen orientations relative to billet orthogonal directions.

Table 2.1. Summary of specimen types, dimensions, which rabbit and the quantity the specimen was included, and measurement performed before and after irradiation.

Specimen Type	Dimensions (mm)	Usage	Measurements
CRS	⌀6 x 8	TTR Creep	Compression strength Dimensions (creep)
CRP	⌀6 x 8 x ⌀1.25	Creep	Dimensions (creep) Compression strength (non-creep)
MB	25 x 3 x 2.9	TTB	Dimensions, mass, Young's modulus, coefficient of thermal expansion (CTE), 4-point flexural strength
TD4	⌀6 x 4	TTR Creep	Thermal conductivity
TD3	⌀6 x 3	TTR Creep	Thermal conductivity

Before irradiation the non-destructive tests were performed on either each specimen, or a subset, for base-line values. The properties considered destructive were the CTE, thermal conductivity, compression strength, and 4-point flexural strength. The CTE and thermal conductivity are potentially destructive if there is a small amount of oxygen in the system resulting in possible oxidation or mass loss. Therefore only a few specimens were tested for these thermal properties and the ones tested were not used for irradiation. Likewise, the strength testing was also destructive, so a small subset of the specimens was used for the baseline measurement. The results of the ORNL-measured as-received physical, mechanical, and thermal properties are summarized in Table 2.2, while complete results of the pre-irradiation measurements are included in "Graphite Pre-Irradiation Specimen Size Validation and Testing Program - Results - Toyo Tanso Japan" [1].

Table 2.2. Physical, mechanical, and thermal properties measured by ORNL on the pre-irradiation specimens.

	Specimen Shape	Orientation	Average ± 1σ
Density (g/cm^3)	All	All	1.77 ± 0.017
Dynamic Young's Modulus (GPa)	MB	AX	9.1 ± 0.23
		TR	9.7 ± 0.22
Compression Strength (MPa)	CRS	AX	77 ± 3.3
		TR	77 ± 2.1
	CRP	AX	75 ± 2.7
		TR	75 ± 3.3
4-point Flexural Strength (MPa)	MB	AX	34 ± 1.8
		TR	36 ± 1.3
Mean CTE at 500°C (10^{-6} K^{-1})	MB	AX	4.5 ± 0.04
		TR	4.2 ± 0.11
Isotropy Ratio			1.057
Thermal Conductivity at 25°C (W/m/K)	TD4	AX	129 ± 7.2
		TR	130 ± 3.7
Thermal Conductivity at 500°C (W/m/K)	TD4	AX	73 ± 3.5
		TR	77 ± 1.4

3. EXPERIMENTAL PROGRAM

3.1 IRRADIATION VEHICLES

The specimens were irradiated in small capsules, called rabbits. Each rabbit consisted of multiple components (Figure 3.1-Figure 3.2) including the housing, specimen holder, specimens, and silicon carbide (SiC). This program utilized two different specimen configurations (TTB and TTR). The small size of these rabbits (nominal 10 mm diameter and 60 mm in length) limited the ability to use on-line measurement techniques, such as thermocouples, and instead SiC was used as a passive temperature monitor. The outer diameter of the specimen holder was varied to get different gas gaps, which were then filled with different inert gasses to achieve the desired specimen temperatures. The necessary gas gap and fill gas was determined by modeling the rabbits in a two-dimensional finite element heat transfer software, and iteratively determining the gap and gas that gave the desired specimen temperature. The ANSYS software was acquired mid-way into this program, which provided the ability to model the rabbits in three-dimensions. At that time, the rabbits were re-modeled in 3D with the parameters from the 2D design. The 3D thermal models for the two rabbit configurations are shown in Figure 3.3.

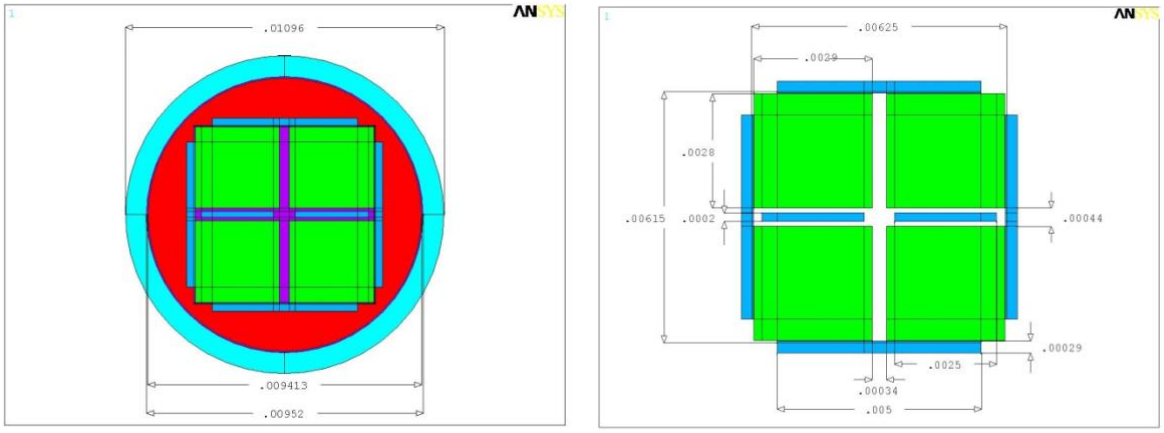

Figure 3.1. Example schematic cross section of a TTB rabbit (from initial 2D thermal design).

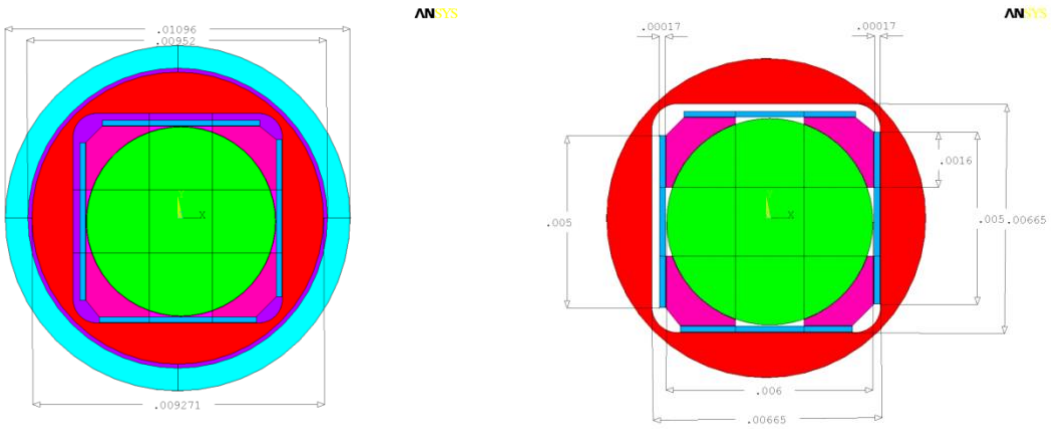

Figure 3.2. Example schematic cross section of a TTR rabbit (from initial 2D thermal design).

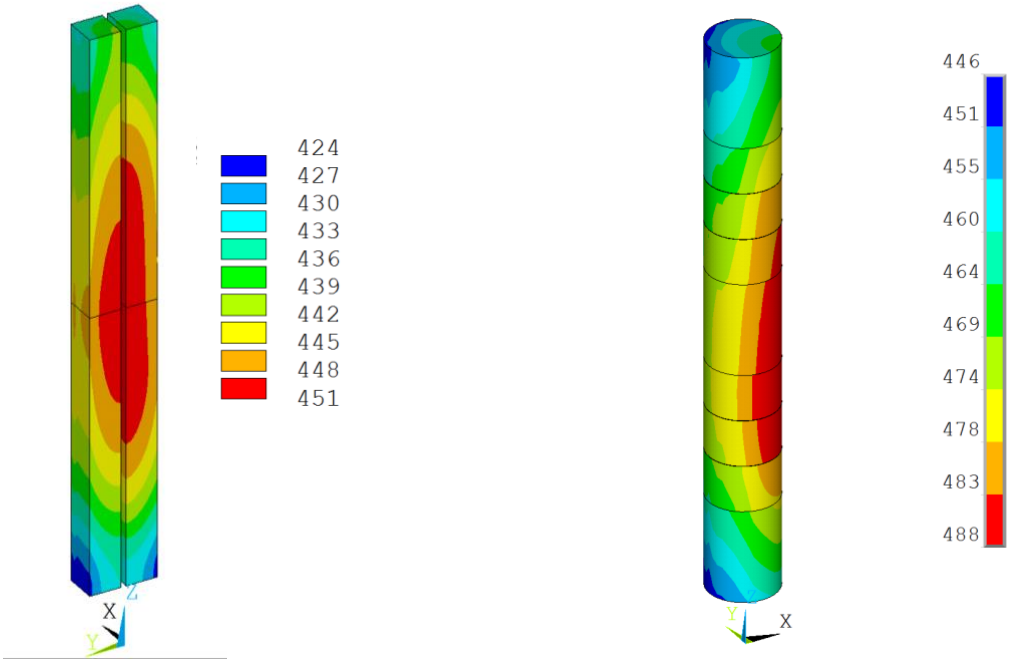

Figure 3.3. 3-dimensions heat-transfer design of the (a) TTB and (b) TTR rabbits.

The objective in planning the irradiation conditions was to achieve temperature and fluence combinations that were relevant to the two high-temperature gas reactor configurations: prismatic core and pebble bed core. The prismatic design has the fuel located within graphite blocks so the graphite will experience higher temperatures, whereas the pebble bed uses graphite for the reflector only so the temperature will be lower. The irradiation behavior of graphite is such that the property changes happen over a much shorter time when the temperature is higher. Therefore, the higher the irradiation temperature, the lower the total fluence that was necessary, which is shown in the planned irradiation envelope in Figure 3.4.

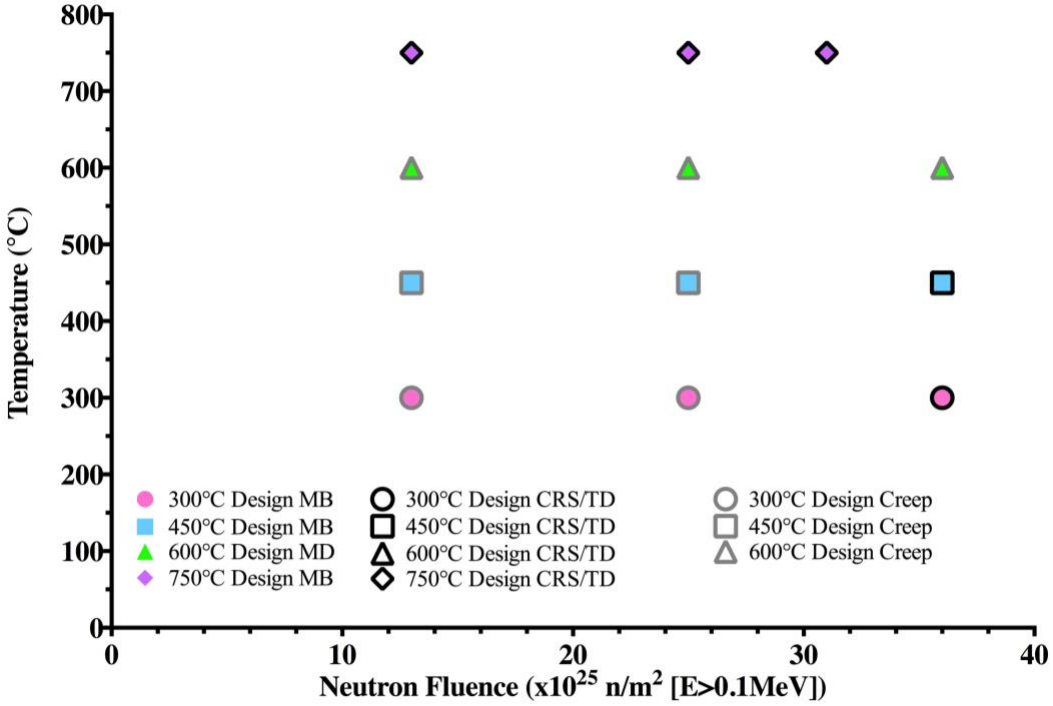

Figure 3.4. Planned irradiation envelope, showing the planned irradiation temperatures and total neutron fluences.

3.2 HFIR INFORMATION

The HFIR at ORNL has one of the highest flux levels available at any materials test reactor in the world. It is an 85 MW pressurized-water reactor, which traditionally operates on approximately a 25-day fuel cycle. The world-leading flux is achieved because the reactor has an annular configuration, schematically shown in Figure 3.5. The central region is the flux trap, which is where the flux levels are highest and where all of this program's specimens were irradiated. The grey region is the fuel, which is then surrounded by the beryllium reflector (purple), control rods (teal), and finally the outer beryllium (green). The rabbits were irradiated in either the peripheral target positions (orange circles in Figure 3.5) or in the outer-most target positions (white hexagons in Figure 3.5 such as B1, C1, A2, or A3). The creep experiments were irradiated in positions E3 and E6, which are the only two flux trap positions able to accommodate experiments that are taller than the pressure vessel. The thermal and fast flux profiles of HFIR, measured in the peripheral target positions and the hydraulic tubes, are plotted in Figure 3.6 versus axial rabbit position (equivalent to location along the height of the core). Along the length of the HFIR core there is room to stack up to 9 rabbits, but traditionally only positions 2-8 are used, with the central positions of 4-6 being preferred because the flux gradient within a rabbit is minimized.

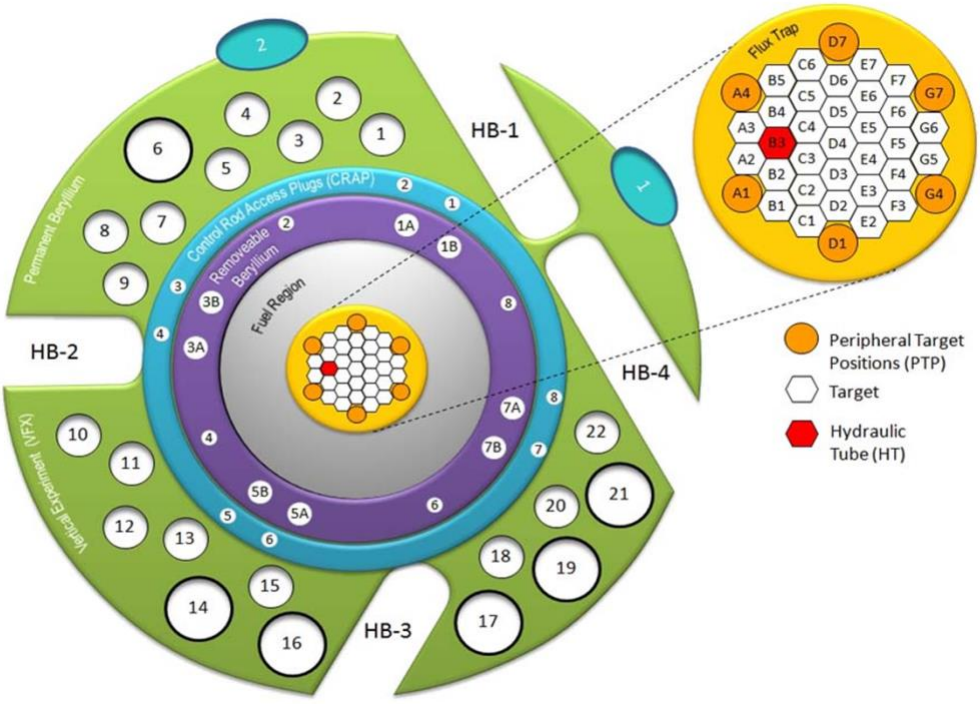

Figure 3.5. Drawing of the HFIR core, where the rabbits were irradiated in the central yellow and white region.

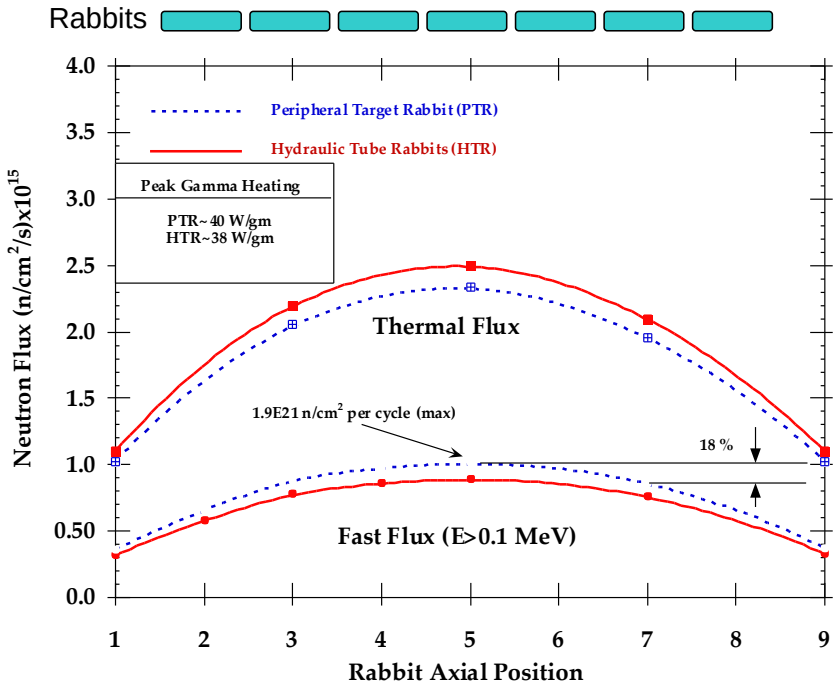

Figure 3.6. Plot of the fast and thermal neutron fluxes versus the rabbit position along the core height (rabbit 1 located at the bottom and rabbit 9 is located at the top). The rabbits in this program were irradiated in positions that correspond to the "Peripheral Target Rabbit" fluxes.

3.3 TEST PROCEDURES

All the pre- and post-irradiation measurements were performed in the LAMDA laboratory. The pre-irradiation measurements were performed in the clean laboratory space in LAMDA according to the Graphite Pre-Irradiation Sample Size Validation and Testing Program [3]. The post-irradiation measurements were performed in the radiation laboratory portion of LAMDA according to the Graphite Post-Irradiation Testing Program – Test Specification [4].

4. RESULTS AND DISCUSSION

4.1 DETERMINING FINAL IRRADIATION CONDITIONS

As was mentioned in Section 3.1, the total fluence and temperature were not directly measured during irradiation. Instead these values were determined via calculations and passive measurement techniques. The flux profiles of HFIR have been measured and modeled numerous times, so the calculation of the total fluence was straightforward. The HFIR is operated at a steady power of 85 MW and when this power can no longer be maintained the reactor is shut down for refueling. The average neutron flux across each rabbit and the total time the rabbit was in the reactor for full-power operation allow for determination of the total fluence of each rabbit.

Active or continuously-monitored thermometry was not used here to monitor temperature during irradiation because of cost and impracticality. Instead, passive silicon carbide coated post-irradiation temperature monitors were used here to determine a single or final temperature of specimens at the end of irradiation [5]. Silicon carbide is an ideal material to use for passive temperature monitoring because the radiation-produced defects will be annealed out at temperatures slightly higher than the irradiation temperature. Therefore, different properties can be measured during a post-irradiation annealing process, and the properties will change once the annealing temperature surpasses the irradiation temperature. The analysis technique used for this program involved determination of the CTE of the SiC as it approached and surpassed the irradiation temperature. It is necessary to note that the SiC results only provide the temperature information for the final two irradiation cycles.

The post-irradiation SiC temperature determination was performed on a dual push-rod dilatometer, and the data used in the analysis is the instantaneous CTE from the heating and cooling segments of the run. An example of the analyzed results is shown in Figure 4.1 for a temperature monitor from the rabbit TTB-01, which had a design temperature of 300°C. In this figure, the heating portion of the dilatometer run is the red data, while the blue data is the cooling segment, and the difference between the two is shown with the purple data. At temperatures below 300°C the heating and cooling behavior are the same, but once the temperature goes above the irradiation temperature the CTE decreases as radiation defects are annealed out of the sample. The process of determining the irradiation temperature has been standardized with a computer program that performs the following steps. 1) A numerical curve is fit to the difference of the heating and cooling curves (s-shaped yellow line). 2) The temperature locations of the first, second and third inflection points of this curve are calculated. 3) Straight lines are fitted to the heating curve at the three inflection points. 4) The temperatures where the straight lines intersect the cooling data are listed as the maximum (black line at first inflection temperature), median (bright blue line at second inflection temperature), and the minimum temperature (green line at third inflection temperature). Additionally, the temperature corresponding to the first inflection point is listed as the transition temperature, because that is the temperature where no new defects are beginning to anneal. The summary of the rabbit information including specimen label, target temperature, target fluence, actual fluence and measured average specimen temperature are shown in Section A.1.

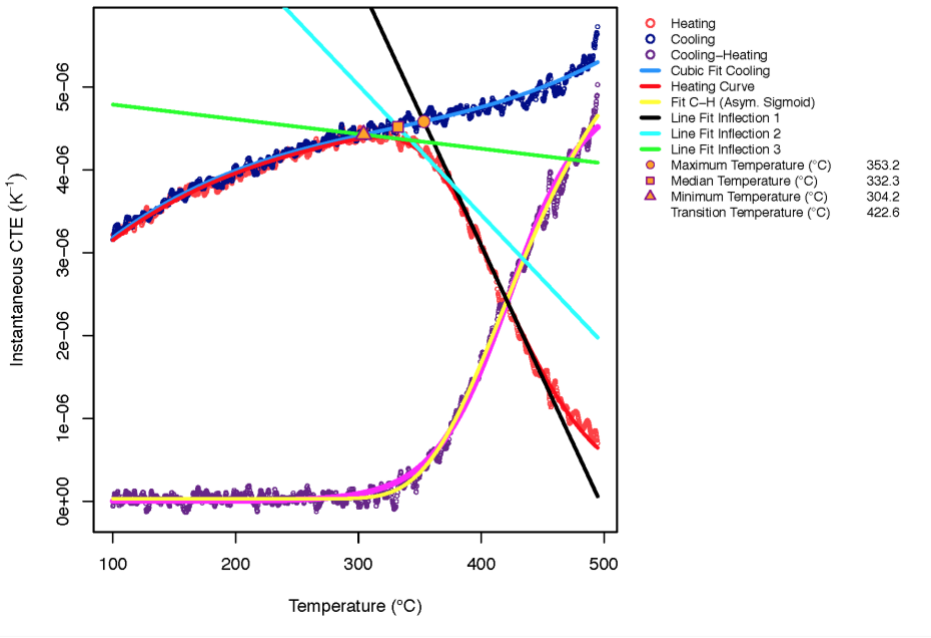

Figure 4.1. Example analysis of passive temperature monitor for rabbit TTB-01.

During the post-irradiation examination campaign, it became apparent that high temperature rabbits did not achieve the design temperature. The rabbits with 750°C target experienced temperatures around 650°C. It was determined that at these high temperatures the heat loss in the axial direction (along the length of the rabbit) is significant and results in higher heat loss than expected. The 2D models of the rabbit cross section underestimated the necessary gas gap width, which resulted in a lower temperature than designed. This was supported by the results from the 3D models of the as-fabricated rabbits which estimated lower temperatures than the initial targets. The final irradiation envelope is plotted in Figure 4.2, where the dashed lines correspond to the target temperatures. The other deviation from planned is the rabbits with the 300°C design temperature. At the intermediate to high fluence (above 20×10^{25} n/m^2 [E>0.1 MeV]) the specimen temperatures were close to 450°C, but these are the same conditions where the changes to the specimens dimensions and thermal conductivity are the greatest, so the rabbit models were not designed to capture these effects.

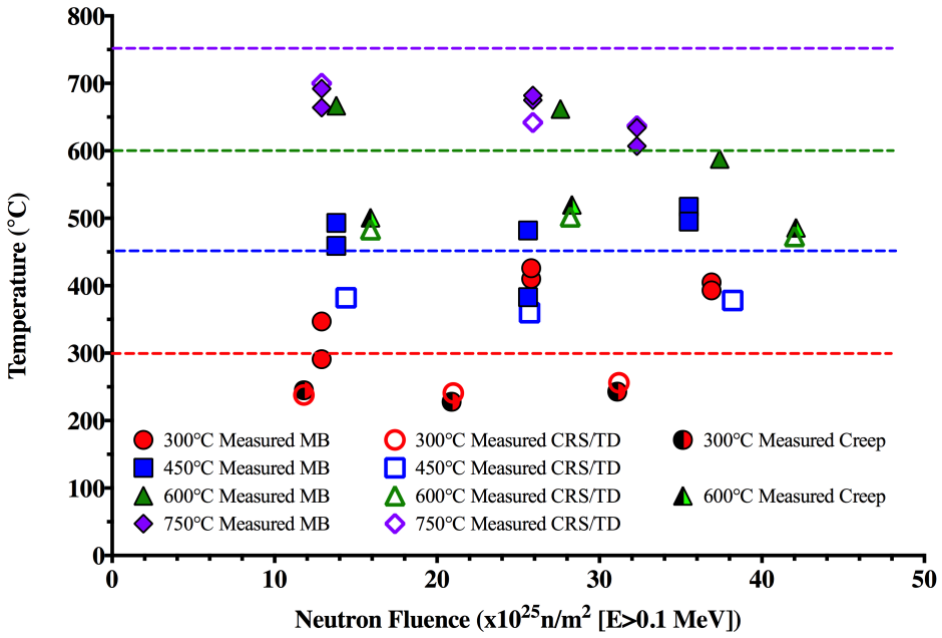

Figure 4.2. Plot of temperature monitor measured temperature and total fluence of each rabbit and creep capsule, where the data points are sorted by shape and color according to the design temperature.

The average specimen temperatures were determined from the 3D thermal model and from the maximum and minimum temperatures from the SiC thermometry. Average temperatures are used for each rabbit since the specimen location within the rabbit was unknown. The specimens were sorted according to target design temperature and the reported temperature ranges are for all specimens from that single target temperature are listed in Table 4.1.

Table 4.1. Grouped specimen temperature, listed as average ±1σ, with temperature range listed in parentheses.

Target Rabbit Temperature (°C)	Unloaded Specimen Temperatures ave. ±1σ (temp. range)	Loaded Specimen Temperatures ave. ±1σ (temp. range)
300	321±74 (238-426)	239±9 (226-253)
450	432±56 (359-517)	n/a
600	554±78 (473-667)	502±15 (481-524)
750	658±29 (607-700)	n/a

As seen in Figure 4.2, the measured temperature for capsules with the same design temperature, but different total fluences are different. The changing specimen dimensions and thermal properties will cause the specimen temperature to change throughout the irradiation time. Within a single HFIR cycle the specimen temperature is not expected to change significantly (due to HFIR power stability), but is expected to change over multiple cycles. An example of a predicted temperature profile, versus irradiation time, is shown in Figure 4.3. The temperature at T_0 is the specimen temperature when irradiation begins. T_1 represents the increase of specimen temperature due to maximum densification when the heat transfer is the lowest. T_2 represents the specimen temperature when the specimen dimensions return to the pre-irradiation values. T_3 is the temperature at the total fluence, where specimens have swelled and heat transfer has increased due to better contact between the specimens and the holder. The 2D and 3D thermal

designs model the specimen temperature at T_2 where the specimen dimensions are the same as pre-irradiation but the thermal properties (CTE and thermal conductivity) are adjusted to expected values from historical irradiation experience (i.e. a thermal conductivity of ~30 W/m/K was used).

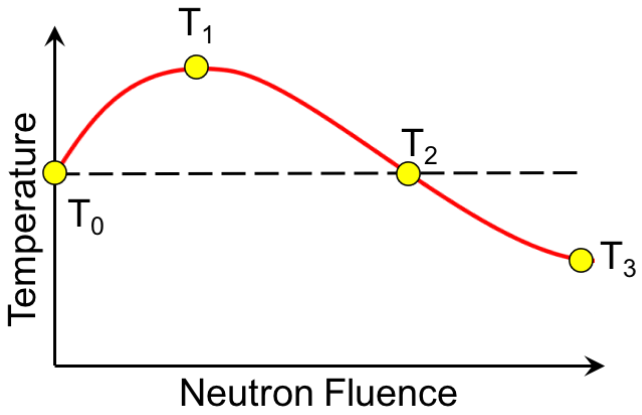

Figure 4.3. Example of possible specimen temperatures versus neutron fluence.

4.2 IRRADIATION-INDUCED CHANGES TO PROPERTIES

The following sections present the results from the measured property changes, sorted by temperature. The first set of plots include the changes in length ($\Delta L/L_0$) (Figure 4.4), volume ($\Delta V/V_0$) (Figure 4.5), Young's modulus ($\Delta E/E_0$) (Figure 4.6), strength ($\Delta S/S_0$) (Figure 4.7 to Figure 4.9), mean CTE at designed temperature with a 25°C reference temperature (Figure 4.10) and thermal conductivity measured at designed temperature (Figure 4.11) plotted versus total neutron fluence. In each plot, the data points represent the average value and the error bars represent one standard deviation, except for volume change where each specimen result is plotted as a single data point. In all the plots, the filled points and solid lines represent AX specimens and the open points and dashed lines are the TR, except for volume change where this distinction is not made. The trend lines shown in all of the plots versus fluence are fitted either with straight lines or polynomials. Please note that these trend lines are only drawn to aid the reader in following the behavior, since there are currently no physical reasons for either type of fit. All of the data used to create these plots are included in the appendices.

The length change results shown in Figure 4.4 only represent the 25 mm length of the MB bars for the plot. This was stipulated based on the precision of the micrometers used and the uncertainty of ~0.1% for the smaller specimen dimensions. The volume change plotted in Figure 4.5 is from only MB specimens.

The compression strength results of the high fluence compression specimens for the 300°C and 450°C design temperatures, presented in the previous report [2], were measured from rod specimens (CRS) irradiated in rabbits. All the other compression results at these design temperatures came from the non-stressed portions of the creep capsules. For consistency it was determined to remove the results from the rabbits from this report and only utilize the specimens that were irradiated in the non-stressed portions of the creep capsules.

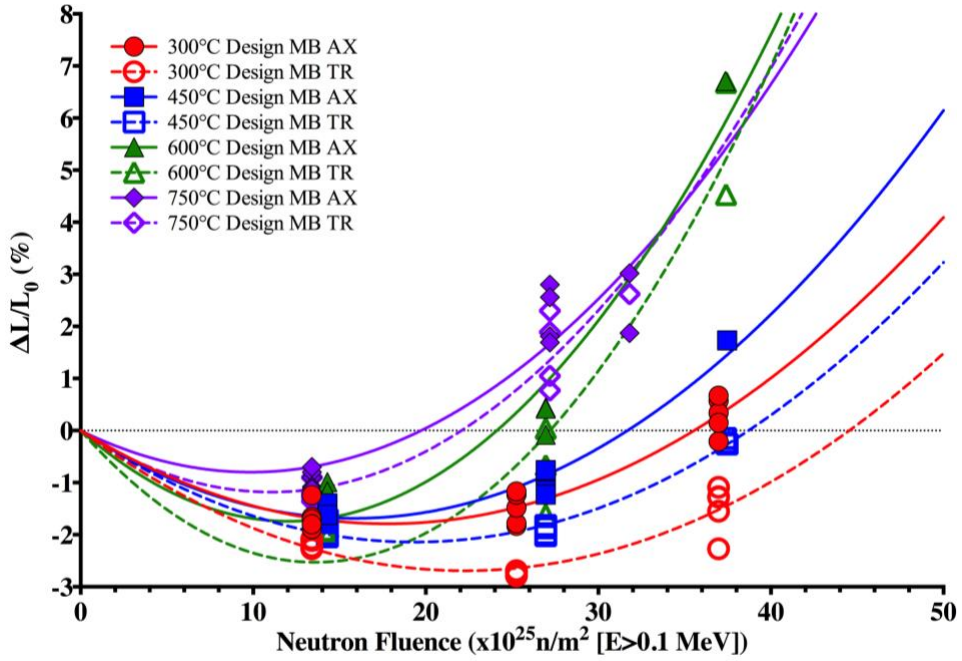

Figure 4.4. Length change of 25 mm dimensions for MB specimens, versus neutron fluence. Points are for each MB specimen measured.

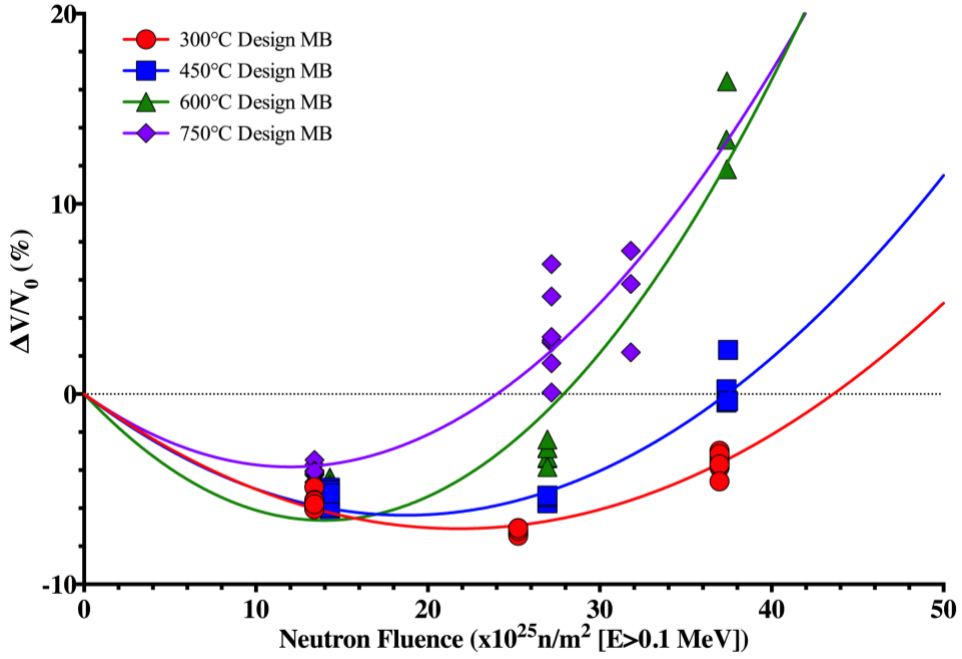

Figure 4.5. Volume change of MB specimens, versus neutron fluence. Points are for each MB specimen measured.

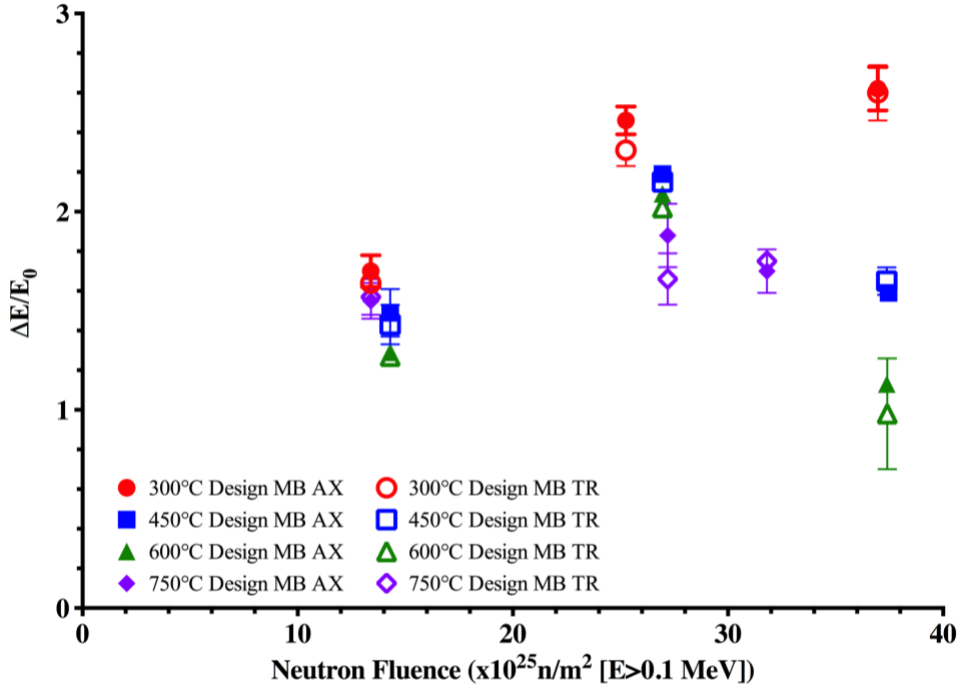

Figure 4.6. Young's modulus change versus neutron fluence. MB values measured via dynamic impulse excitation. Points are average ±1σ, but in some cases standard deviation is smaller than size of data point.

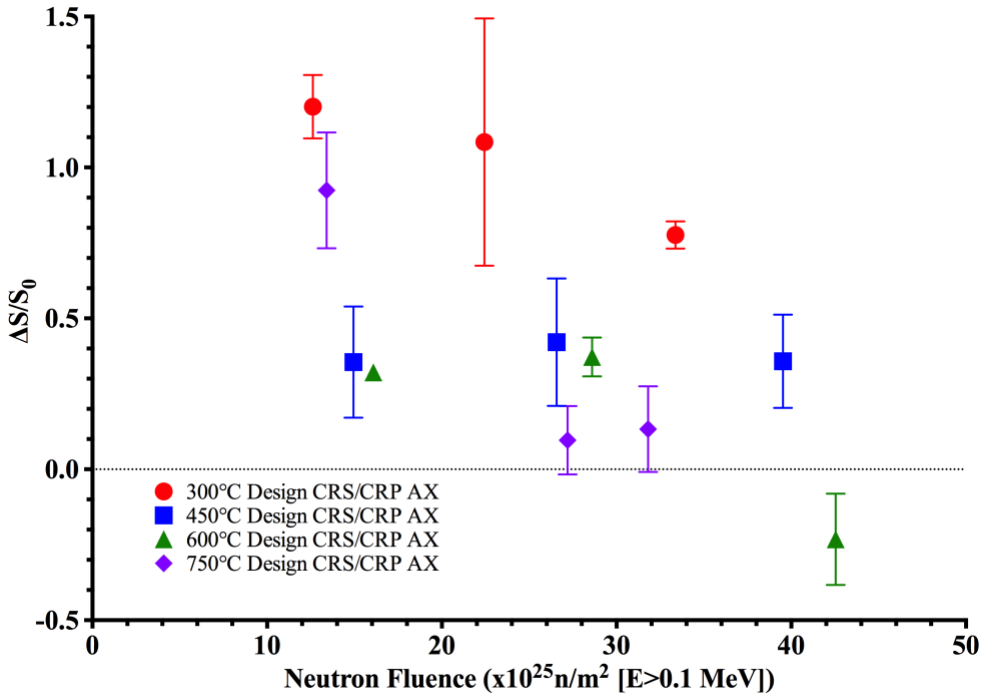

Figure 4.7. Compression strength change, versus neutron fluence. All results from CRS/CRP specimens in unstressed region of creep experiment except 750°C. Points are average ±1σ.

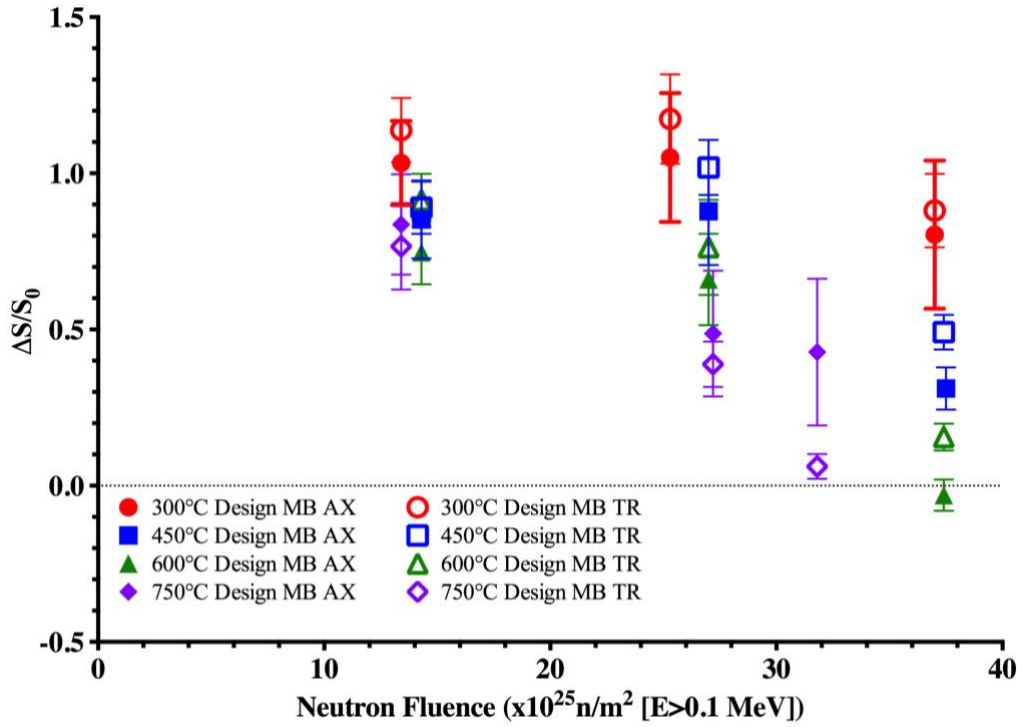

Figure 4.8. 4-point flexural strength change of MB specimens, versus neutron fluence. Points are average ±1σ.

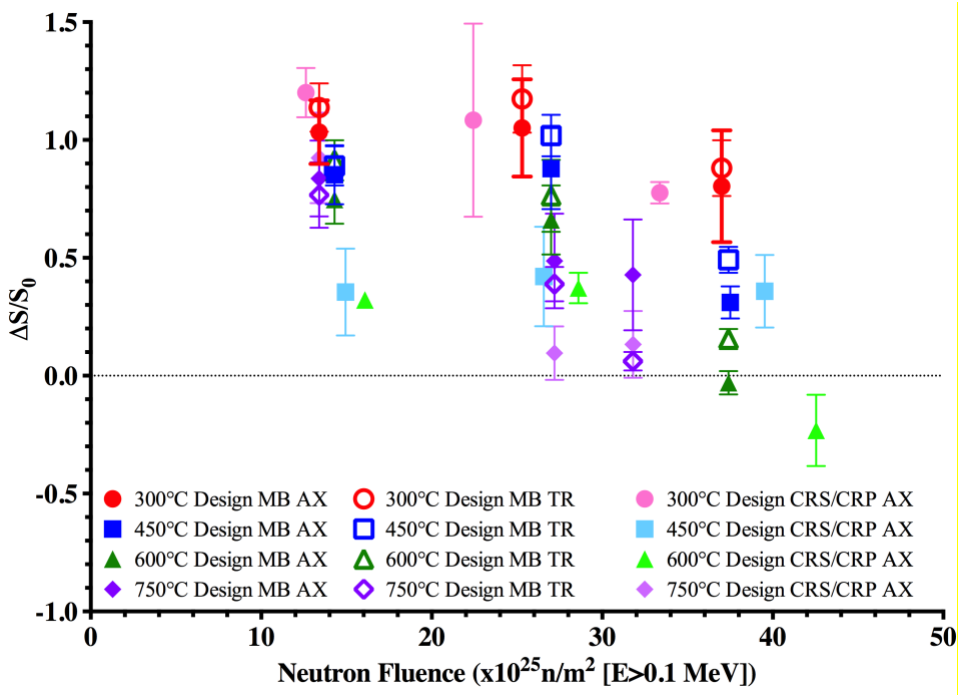

Figure 4.9. Strength change comparison for two different strength measurements (4-point flexural from MB specimens and compression from CRS/CRP specimens), versus neutron fluence. Points are average ±1σ.

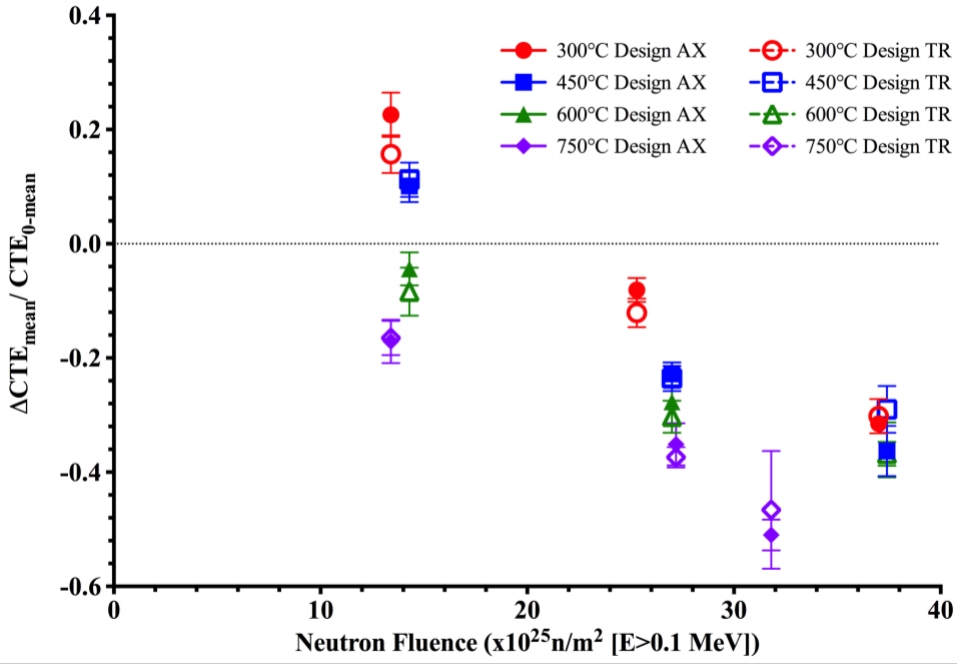

Figure 4.10. Change of mean CTE at target irradiation temperature, versus neutron fluence. Points are average ±1σ, but in some cases standard deviation is smaller than size of data point.

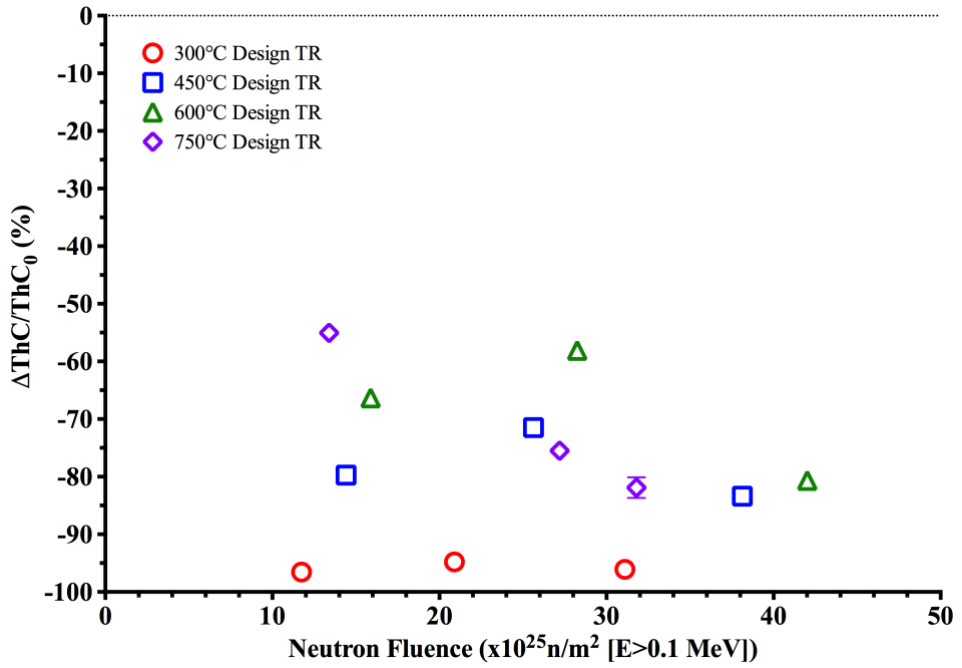

Figure 4.11. Change of thermal conductivity versus neutron fluence. Points are average ±1σ, but standard deviation is smaller than size of data point.

4.3 IRRADIATION-INDUCED CREEP

The post-irradiation examination of the irradiation-induced creep experiments was completed, and the results are summarized in this section. The creep experiment had two distinct temperature regions: 300°C, and 600°C. The applied compressive stress was nominally 13.5 MPa. Unlike the rabbits, the design of these experiments was very complex. The final average specimen temperatures achieved for these regions were 243°C and 497°C, respectively. The results of the dimensional change of the stressed specimens are shown in Figure 4.12.

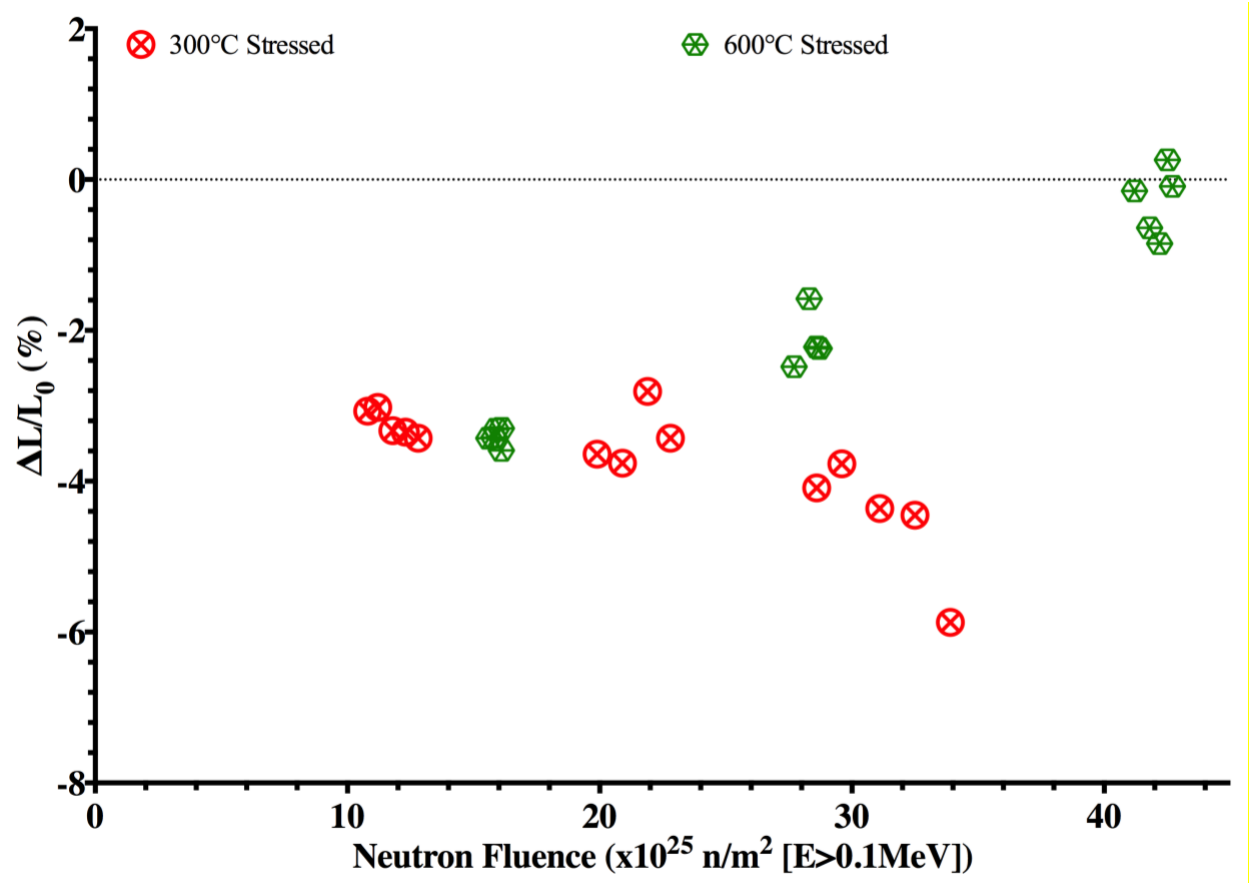

Figure 4.12. Dimensional strain of stressed specimens in creep capsules.

4.4 HISTORICAL BEHAVIOR COMPARISON

In the American Society of Mechanical Engineers (ASME) code for high temperature reactors [6], article HAB-7000, lists the ASTM standards that cover the pre-irradiation specifications for nuclear graphite. These standards include ASTM D7219 [7] and ASTM D7301 [8]. In D7219 (relevant for IG-110), the CTE isotropy ratio must be less than 1.1, a density above 1.7 g/cm^3, room temperature thermal conductivity of 90 W/m/K, Young's modulus between 8-15 GPa, and tensile, flexural, and compressive strengths, greater than 22, 35, and 65 MPa, respectively. The properties measured by ORNL all fell within the acceptable limits to quantify IG-110 as nuclear grade graphite.

More importantly is the fact that IG-110 has exhibited the same irradiation response that has been observed since the 1960's when results on irradiation effects in graphite were first published. Many programs have studied the effect of irradiation on medium and large grained graphites that were either pressed or extruded [9-24]. All of these programs observed similar trends, even for different grades of graphite. These trends include: the difference in length change relative to the with- or against-grain orientation, an increase of Young's modulus to a peak value that then decreased to an elevated plateau, a rapid rise in the electrical resistivity followed by a plateau, strength increased and then decreased, thermal conductivity underwent sharp decrease to a plateau value, and a peak of CTE followed by a decrease to a plateau. In work with varied irradiation temperature, [15-17, 20, 24], it was found that these changes happened more rapidly at higher irradiation temperatures but the severity of the changes were reduced.

Unlike the previous research, this program has been much more comprehensive in the temperature/fluence levels investigated, and the properties measured. This comprehensiveness allows for a more rigorous investigation into the effects of temperature and fluence on the different physical, mechanical, and thermal properties. The only un-expected behavior is shown in the length change, since it has been a commonly held belief that near-isotropic isostatically pressed graphite will have the same property change in all directions. Instead this work shows this belief to be incorrect for IG-110, so for irradiation-induced property changes it is imperative for investigation to look at property changes in both distinct directions. Otherwise all the other trends show the same types of behaviors that have been observed in the past with other graphite.

The most significant contribution from this program is that it is one of the most comprehensive investigations of the effect of irradiation temperature and neutron fluence on a single graphite grade. An example of the comprehensiveness is the results of neutron fluence and temperature on two different strengths (Figure 4.9). In previous work, traditionally only one type of strength was measured for post-irradiation changes, but this work included changes to both flexural and compressive strengths. These results have confirmed the belief that measuring one type of strength change should be sufficient to predict the changes that will result for the other strengths, so the ASME Boiler and Pressure Vessel code for high temperature reactors [6] requirement of only measuring one strength change is supported.

5. QUALITY ASSURANCE DOCUMENTATION

The ORNL quality assurance systems and processes used to plan, conduct, and document the subject activities are described in ORNL document # QAP-ORNL-NR&D-01 entitled *Quality Assurance Plan for Nuclear Research and Development Conducted at the Oak Ridge National Laboratory.* This document describes the management system implemented to assure the quality of the work performed for nuclear research endeavors, including the Tokai -funded nuclear science and technology activities at ORNL. The plan is explicitly formulated to identify the ORNL and project-level documents utilized to address the body of requirements associated with the quality standard, ANSI/ISO/ASQ Q9001-2008 entitled *American National Standard – Quality Management Systems - Requirements* (hereafter referred to as ISO 9001) as it applies to the scope of work. The ORNL has been registered to the ISO 9001 standard since 2010 and undergoes annual audits to maintain its registration. The ORNL's Metrology organization is also accredited to the ISO 17025 standard entitled *General Requirements for the Competence of Testing and Calibration Laboratories.*

In addition to the ISO 9001 standard, other documents form a set of references that – in part – are included as inputs to the nuclear Research & Development Quality Assurance plan because they are 1) customer-mandated requirements, 2) have been previously useful in achieving and documenting success in nuclear Science & Technology-related activities, or 3) because they are an explicit component of the requirements set incumbent upon ORNL as a United States Department of Energy (DOE) site.

- ASME NQA-1-2008, *Quality Assurance Requirements for Nuclear Facility Applications*
- ASME NQA-1-2008, Part IV, Subpart 4.2, *Guidance on Graded Application of Quality Assurance (QA) for Nuclear Related Research and Development*, and Subpart 4.3, *Modification of an ISO 9001-2000 Quality Program to Meet NQA-1-2000 Requirements*
- DOE Guide 414.1-2, *Quality Assurance Management System Guide for Use with 10 CFR 830.120 and DOE O 414.1C*
- ORNL Quality Assurance Program Description

6. SUMMARY

The results presented in the document represent one of the most comprehensive graphite irradiation campaigns. This campaign investigated a range of temperatures and fluence that are relevant to both the prismatic and pebble bed core High-Temperature Gas-Cooled Reactors and it also provided a thorough investigation into the effects of the irradiation temperature and fast neutron fluence on multiple physical, mechanical, and thermal properties.

Specimens machined from IG-110 were irradiated in the ORNL HFIR in specially designed irradiation capsules. The capsules were designed to irradiate the specimens at target temperatures of 300, 450°C, 600°C, and 750°C. It was determined that the intended target temperatures for the 750°C capsules were not obtained due to higher than expected heat loss along the length of the capsules. The maximum fast neutron fluence obtained was ~36×10^{25} n/m^2 [E>0.1MeV] (~26 dpa). From these capsules, the irradiation-induced changes to the specimen dimensions, Young's modulus, strength, coefficient of thermal expansion, and thermal conductivity were determined. The changes that occurred in these properties of IG-110 agree with the trends that have historically been observed in literature for other nuclear graphite.

7. REFERENCES

1. Snead, M.A., J. Robertson, and Y. Katoh, "Graphite Pre-Irradiation Specimen Size Validation and Testing Program - Results - Toyo Tanso Japan", ORNL/TM-2017/140, (2017).
2. Campbell, A.A. and Y. Katoh, "Report on Effects of Irradiation on Material IG-110 -Prepared for Toyo Tanso Co., Ltd.", ORNL/TM-2017/705, (2017).
3. Snead, M.A. and Y. Katoh, "Graphite Pre-Irradiation Sample Size Validation and Testing Program – Test Specification – Toyo Tanso Japan", ORNL/TM-2014/231, (2011).
4. Snead, M.A. and Y. Katoh, "Graphite Post-Irradiation Testing Program – Test Specification – Toyo Tanso Japan", ORNL/TM-2014/231, (2014).
5. Campbell, A.A., W.D. Porter, Y. Katoh, and L.L. Snead, "Method for Analyzing Passive SiC Thermometry with a Continuous Dilatometer to Determine Irradiation Temperature", *NIMB*, 370, (2016) 49-58.
6. ASME III-5, 2017, "ASME Boiler and Pressure Vessel Code An International Code", New York, NY,
7. ASTM D7219-08 (2014), 2014, "Standard Specification for Isotropic and Near-Isotropic Nuclear Graphites", ASTM International, West Conshohocken, PA, DOI: 10.1520/D7219-08R14, www.astm.org.
8. ASTM D7301-11, 2011, "Standard Specification for Nuclear Graphite Suitable for Components Subjected to Low Neutron Irradiation Dose", ASTM International, West Conshohocken, PA, 10.1520/D7301-11R15, www.astm.org.
9. Nightingale, R.E., "Nuclear Graphite", 1962, New York, Academic Press.
10. Kelly, B.T., D. Jones, and A. James, "Irradiation damage to pile grade graphite at 450° C", *Journal of Nuclear Materials*, 7, (1962) 279-291.
11. Bridge, H., B.T. Kelly, and P.T. Nettley, "Effect of high-flux fast-neutron irradiation on the physical properties of graphite", *Carbon*, 2, (1964) 83-93.
12. Simmons, J.H.W., B.T. Kelly, P.T. Nettley, and W.N. Reynolds, "The Irradiation Behavior of Graphite", Proceedings of the Third United Nations Internatinal Conference on the Peaceful Uses of Atomic Energy, United Kingdon, 1964, Paper #163.
13. Kelly, B.T., W.H. Martin, and P.T. Nettley, "Dimensional Changes in Polycrystalline Graphites under Fast-Neutron Irradiation", *Philosophical Transactions of the Royal Society A*, 260, (1966) 51-71.
14. Nettley, P.T., J.E. Brocklehurst, W.H. Martin, and J.H.W. Simmons, "Irradiation Experience with Isotropic Graphite", Presented at *Symposium on Advanced and High Temperature Gas-Coolet Reactors*, Julich, October 21-25, 1968.
15. Simmons, J.H.W., "Radiation damage in graphite", International Series of Monographs in Nuclear Energy, Vol. 102, 1965, Oxford, New York, Pergamon Press.
16. Kelly, B.T., "Physics of Graphite", 1981, London, Applied Science Publishers.
17. Burchell, T.D. and W.P. Eatherly, "The effects of radiation damage on the properties of GraphNOL N3M", *Journal of Nuclear Materials*, 179-181, Part 1, (1991) 205-208.
18. "Irradiation Damage in Graphite due to Fast Neutrons in Fission and Fusion Systems", IAEA-TECDOC-1154, (2000).
19. Burchell, T.D., "Neutron Irradiation Damage in Graphite and Its Effects on Properties", Presented at *International Carbon Conference CARBON 2002*, Beijing, China, September 15-20, 2002.
20. Haag, G., "Properties of ATR-2E Graphite and Property Changes due to Fast Neutron Irradiation", Berichte des Forschungszentrums J\'fclich\, Vol. 4183\, 2005, J\'fclich\, FZJ, Institut f\'fcr Sicherheitsforschung und Reaktortechnik\.
21. Burchell, T.D. and L.L. Snead, "The effect of neutron irradiation damage on the properties of grade NBG-10 graphite", *Journal of Nuclear Materials*, 371, (2007) 18-27.
22. Burchell, T.D., "4.10 - Radiation Effects in Graphite", in *Comprehensive Nuclear Materials*, R.J.M. Konings, Editor, 2012, Elsevier, Oxford, p. 299-324.

23. Ishiyama, S., T.D. Burchell, J.P. Strizak, and M. Eto, "The effect of high fluence neutron irradiation on the properties of a fine-grained isotropic nuclear graphite", *Journal of Nuclear Materials*, 230, (1996) 1-7.
24. Kelly, B.T. and T.D. Burchell, "Structure-related property changes in polycrystalline graphite under neutron irradiation", *Carbon*, 32, (1994) 499-505.

APPENDIX A. RABBIT INFORMATION

A.1 IRRADIATION RESULTS SUMMARY

Capsule ID	Target Temperature (°C)	Target Fluence ($x10^{25}$ n/m^2 [E>0.1MeV])	Actual Fluence ($x10^{25}$ n/m^2 [E>0.1MeV])	Measured Average Specimen Temperature (°C)
TTR-03	750	13	12.9	700
TTR-04	750	25	25.9	642
TTR-05	750	31	32.3	637
TTB-01	300	13	12.9	347
TTB-02	300	13	12.9	291
TTB-03	300	25	25.8	410
TTB-04	300	25	25.8	426
TTB-05	300	36	36.9	405
TTB-06	300	36	36.9	393
TTB-07	450	13	13.8	459
TTB-08	450	13	13.8	493
TTB-09	450	25	25.6	482
TTB-10	450	25	25.6	383
TTB-11	450	36	35.5	517
TTB-12	450	36	35.5	495
TTB-13	600	13	13.8	667
TTB-14	600	25	27.6	662
TTB-15	600	36	37.4	588
TTB-16	750	13	12.9	664
TTB-17	750	13	12.9	692
TTB-18	750	25	25.9	675
TTB-19	750	25	25.9	682
TTR-20	750	31	32.3	607
TTB-21	750	31	32.3	634
TTC-3-1	300	13	11.8	245
TTC-3-3	600	13	15.9	501
TTC-3-4	600	13	15.9	483
TTC-3-5	450	13	14.4	382
TTC-3-6	300	13	11.8	238
TTC-2-1	300	25	20.9	228
TTC-2-3	600	25	28.3	520
TTC-2-4	600	25	28.2	502
TTC-2-5	450	25	25.7	360
TTC-2-6	300	25	21.0	241
TTC-1-1	300	36	31.1	243
TTC-1-3	600	36	42.1	486
TTC-1-4	600	36	42.0	473
TTC-1-5	450	36	38.2	378
TTC-1-6	300	36	31.2	256

APPENDIX B. SPECIMEN RESULTS

B.1 POST-IRRADIATION DIMENSION AND YOUNG'S MODULUS

ID	Material	Sample Type	Orien.	Design Temp. (°C)	Measured Temp. (°C)	Neutron Fluence ($x10^{25}$ n/m^2 [E>0.1 MeV])	Volume Change ($\Delta V/V_0$)	Length Change ($\Delta L/L_0$)	Young's Change ($\Delta E/E_0$)
T10A00	IG110	MB	AX	300	347	13.4	-6.04%	-1.89%	1.76
T10A01	IG110	MB	AX	300	347	13.4	-4.90%	-1.24%	1.59
T10A02	IG110	MB	AX	300	347	13.4	-5.57%	-1.66%	1.65
T10A03	IG110	MB	AX	300	291	13.4	-5.71%	-1.70%	1.70
T10A04	IG110	MB	AX	300	291	13.4	-6.04%	-1.80%	1.80
T10A05	IG110	MB	AX	300	410	25.3	-7.24%	-1.83%	2.40
T10A06	IG110	MB	AX	300	410	25.3	-7.33%	-1.78%	2.39
T10A07	IG110	MB	AX	300	410	25.3	-7.19%	-1.48%	2.45
T10A08	IG110	MB	AX	300	426	25.3	-7.10%	-1.23%	2.48
T10A09	IG110	MB	AX	300	426	25.3	-7.04%	-1.17%	2.60
T10A10	IG110	MB	AX	300	405	37.0	-3.48%	0.57%	2.70
T10A11	IG110	MB	AX	300	405	37.0	-3.28%	0.34%	2.60
T10A12	IG110	MB	AX	300	405	37.0	-3.03%	0.67%	2.43
T10A13	IG110	MB	AX	300	393	37.0	-3.62%	-0.21%	2.63
T10A14	IG110	MB	AX	300	393	37.0	-3.86%	0.15%	2.73
T10T00	IG110	MB	TR	300	347	13.4	-5.85%	-2.24%	1.64
T10T01	IG110	MB	TR	300	347	13.4	-5.74%	-2.08%	1.61
T10T02	IG110	MB	TR	300	347	13.4	-6.05%	-2.27%	1.72
T10T03	IG110	MB	TR	300	291	13.4	-5.61%	-2.23%	1.61
T10T69	IG110	MB	TR	300	291	13.4	-5.79%	-2.11%	1.64
T10T05	IG110	MB	TR	300	410	25.3	-7.14%	-2.72%	2.45
T10T06	IG110	MB	TR	300	410	25.3	-7.39%	-2.79%	2.28
T10T07	IG110	MB	TR	300	410	25.3	-7.45%	-2.71%	2.31
T10T08	IG110	MB	TR	300	426	25.3	-7.19%	-2.69%	2.29
T10T09	IG110	MB	TR	300	426	25.3	-7.05%	-2.72%	2.22
T10T10	IG110	MB	TR	300	405	37.0	-3.72%	-2.27%	2.51
T10T11	IG110	MB	TR	300	405	37.0	-2.98%	-1.55%	2.54
T10T12	IG110	MB	TR	300	405	37.0	-3.15%	-1.28%	2.46
T10T13	IG110	MB	TR	300	393	37.0	-3.70%	-1.27%	2.62
T10T14	IG110	MB	TR	300	393	37.0	-4.59%	-1.09%	2.87
T10A15	IG110	MB	AX	450	459	14.3	-5.89%	-1.51%	1.62
T10A16	IG110	MB	AX	450	459	14.3	-6.02%	-1.60%	1.59
T10A17	IG110	MB	AX	450	459	14.3	-5.99%	-1.61%	1.54
T10A18	IG110	MB	AX	450	493	14.3	-4.92%	-1.40%	1.33
T10A19	IG110	MB	AX	450	493	14.3	-5.34%	-1.62%	1.34
T10A20	IG110	MB	AX	450	482	27.0	-5.74%	-0.88%	2.25
T10A21	IG110	MB	AX	450	482	27.0	-5.45%	-0.97%	2.19
T10A22	IG110	MB	AX	450	482	27.0	-5.43%	-0.76%	2.21
T10A23	IG110	MB	AX	450	383	27.0	-5.61%	-1.15%	2.16
T10A24	IG110	MB	AX	450	383	27.0	-5.52%	-1.23%	2.16
T10A28	IG110	MB	AX	450	495	37.5	2.32%	1.73%	1.59
T10T15	IG110	MB	TR	450	459	14.3	-6.02%	-2.04%	1.51
T10T16	IG110	MB	TR	450	459	14.3	-6.11%	-2.00%	1.53
T10T17	IG110	MB	TR	450	459	14.3	-5.96%	-2.04%	1.51
T10T18	IG110	MB	TR	450	493	14.3	-5.06%	-1.71%	1.30
T10T19	IG110	MB	TR	450	493	14.3	-5.22%	-1.77%	1.32
T10T20	IG110	MB	TR	450	482	27.0	-5.62%	-1.85%	2.11
T10T21	IG110	MB	TR	450	482	27.0	-5.66%	-1.87%	2.13
T10T22	IG110	MB	TR	450	482	27.0	-5.74%	-1.98%	2.13
T10T23	IG110	MB	TR	450	383	27.0	-5.42%	-2.02%	2.16
T10T24	IG110	MB	TR	450	383	27.0	-5.34%	-1.82%	2.19
T10T26	IG110	MB	TR	450	517	37.4	0.25%	-0.15%	1.60

ID	Material	Sample Type	Orien.	Design Temp. (°C)	Measured Temp. (°C)	Neutron Fluence ($x10^{25}$ n/m^2 [E>0.1 MeV])	Volume Change ($\Delta V/V_0$)	Length Change ($\Delta L/L_0$)	Young's Change ($\Delta E/E_0$)
T10T27	IG110	MB	TR	450	517	37.4	-0.44%	-0.23%	1.60
T10T28	IG110	MB	TR	450	495	37.5	-0.38%	-0.26%	1.75
T10A30	IG110	MB	AX	600	667	14.3	-4.39%	-1.21%	1.30
T10A31	IG110	MB	AX	600	667	14.3	-4.42%	-0.99%	1.27
T10A32	IG110	MB	AX	600	667	14.3	-4.81%	-1.17%	1.29
T10A33	IG110	MB	AX	600	662	27.0	-3.37%	0.44%	2.11
T10A34	IG110	MB	AX	600	662	27.0	-3.33%	0.42%	2.08
T10A35	IG110	MB	AX	600	662	27.0	-3.83%	-0.08%	2.08
T10A36	IG110	MB	AX	600	588	37.4	13.38%	6.71%	1.13
T10T30	IG110	MB	TR	600	667	14.3	-4.74%	-1.91%	1.27
T10T31	IG110	MB	TR	600	667	14.3	-5.07%	-2.03%	1.27
T10T32	IG110	MB	TR	600	667	14.3	-4.96%	-1.94%	1.26
T10T33	IG110	MB	TR	600	662	27.0	-2.82%	-1.62%	1.97
T10T34	IG110	MB	TR	600	662	27.0	-2.85%	-0.67%	2.03
T10T35	IG110	MB	TR	600	662	27.0	-2.39%	0.04%	2.07
T10T37	IG110	MB	TR	600	588	37.4	16.44%	6.68%	0.70
T10T38	IG110	MB	TR	600	588	37.4	11.83%	4.53%	1.25
T10A39	IG110	MB	AX	750	664	13.4	-4.26%	-0.90%	1.62
T10A40	IG110	MB	AX	750	664	13.4	-4.19%	-0.80%	1.64
T10A41	IG110	MB	AX	750	664	13.4	-4.04%	-0.70%	1.61
T10A42	IG110	MB	AX	750	692	13.4	-4.62%	-1.08%	1.45
T10A43	IG110	MB	AX	750	692	13.4	-4.65%	-1.12%	1.45
T10A45	IG110	MB	AX	750	675	27.2	1.62%	1.81%	1.97
T10A46	IG110	MB	AX	750	675	27.2	0.08%	1.69%	2.09
T10A47	IG110	MB	AX	750	682	27.2	2.82%	2.80%	1.72
T10A48	IG110	MB	AX	750	682	27.2	2.70%	2.56%	1.74
T10A50	IG110	MB	AX	750	607	31.8	5.79%	3.02%	1.60
T10A52	IG110	MB	AX	750	634	31.8	2.19%	1.87%	1.81
T10T39	IG110	MB	TR	750	664	13.4	-3.71%	-1.22%	1.64
T10T40	IG110	MB	TR	750	664	13.4	-3.46%	-0.90%	1.70
T10T41	IG110	MB	TR	750	664	13.4	-4.03%	-1.18%	1.57
T10T42	IG110	MB	TR	750	692	13.4	-4.11%	-1.28%	1.50
T10T43	IG110	MB	TR	750	692	13.4	-4.07%	-1.36%	1.47
T10T45	IG110	MB	TR	750	675	27.2	6.83%	2.30%	1.47
T10T46	IG110	MB	TR	750	675	27.2	5.13%	1.89%	1.61
T10T47	IG110	MB	TR	750	682	27.2	2.83%	0.77%	1.79
T10T48	IG110	MB	TR	750	682	27.2	3.00%	1.05%	1.77
T10T52	IG110	MB	TR	750	634	31.8	7.53%	2.62%	1.75

B.2 POST-IRRADIATION COEFFICIENT OF THERMAL EXPANSION

ID	Material	Sample Type	Orien.	Design Temp. (°C)	Measured Temp. (°C)	Neutron Fluence ($x10^{25}$ n/m^2 [E>0.1 MeV])	CTE Change ($\Delta\alpha/\alpha_0$) (at design temperature)
T10A00	IG110	MB	AX	300	347	13.4	17.7%
T10A03	IG110	MB	AX	300	291	13.4	22.9%
T10A04	IG110	MB	AX	300	291	13.4	19.7%
T10A05	IG110	MB	AX	300	410	25.3	-10.7%
T10A06	IG110	MB	AX	300	410	25.3	-6.6%
T10A07	IG110	MB	AX	300	410	25.3	-7.1%
T10A10	IG110	MB	AX	300	405	37.0	-31.7%
T10A11	IG110	MB	AX	300	405	37.0	-30.5%
T10A12	IG110	MB	AX	300	405	37.0	-32.2%
T10T00	IG110	MB	TR	300	347	13.4	15.0%
T10T03	IG110	MB	TR	300	291	13.4	16.2%
T10T69	IG110	MB	TR	300	291	13.4	16.0%
T10T05	IG110	MB	TR	300	410	25.3	-12.3%
T10T06	IG110	MB	TR	300	410	25.3	-12.8%
T10T07	IG110	MB	TR	300	410	25.3	-11.3%
T10T12	IG110	MB	TR	300	405	37.0	-33.5%
T10T13	IG110	MB	TR	300	393	37.0	-28.9%
T10T14	IG110	MB	TR	300	393	37.0	-28.1%
T10A15	IG110	MB	AX	450	459	14.3	13.8%
T10A16	IG110	MB	AX	450	459	14.3	8.8%
T10A17	IG110	MB	AX	450	459	14.3	7.7%
T10A20	IG110	MB	AX	450	482	27.0	-24.0%
T10A21	IG110	MB	AX	450	482	27.0	-24.3%
T10A22	IG110	MB	AX	450	482	27.0	-20.2%
T10A25	IG110	MB	AX	450	517	37.4	-40.4%
T10A27	IG110	MB	AX	450	517	37.4	-38.3%
T10A29	IG110	MB	AX	450	495	37.5	-30.2%
T10T15	IG110	MB	TR	450	459	14.3	9.8%
T10T16	IG110	MB	TR	450	459	14.3	11.6%
T10T17	IG110	MB	TR	450	459	14.3	12.2%
T10T20	IG110	MB	TR	450	482	27.0	-24.0%
T10T21	IG110	MB	TR	450	482	27.0	-24.8%
T10T22	IG110	MB	TR	450	482	27.0	-22.1%
T10T25	IG110	MB	TR	450	517	37.4	-25.6%
T10T28	IG110	MB	TR	450	495	37.5	-27.2%
T10T29	IG110	MB	TR	450	495	37.5	-34.2%
T10A31	IG110	MB	AX	600	667	14.3	-6.1%
T10A30	IG110	MB	AX	600	667	14.3	-6.5%
T10A32	IG110	MB	AX	600	667	14.3	-0.5%
T10A33	IG110	MB	AX	600	662	27.0	-31.0%
T10A34	IG110	MB	AX	600	662	27.0	-29.9%
T10A35	IG110	MB	AX	600	662	27.0	-22.1%
T10A36	IG110	MB	AX	600	588	37.4	-40.8%
T10A38	IG110	MB	AX	600	588	37.4	-38.1%
T10A37	IG110	MB	AX	600	588	37.4	-29.5%
T10T30	IG110	MB	TR	600	667	14.3	-12.1%
T10T31	IG110	MB	TR	600	667	14.3	-9.7%
T10T32	IG110	MB	TR	600	667	14.3	-3.6%
T10T33	IG110	MB	TR	600	662	27.0	-32.8%
T10T34	IG110	MB	TR	600	662	27.0	-30.9%
T10T35	IG110	MB	TR	600	662	27.0	-27.3%
T10T36	IG110	MB	TR	600	588	37.4	-34.8%
T10T37	IG110	MB	TR	600	588	37.4	-37.6%
T10T38	IG110	MB	TR	600	588	37.4	-38.0%
T10A39	IG110	MB	AX	750	664	13.4	-21.9%

ID	Material	Sample Type	Orien.	Design Temp. (°C)	Measured Temp. (°C)	Neutron Fluence ($x10^{25}$ n/m^2 [E>0.1 MeV])	CTE Change ($\Delta\alpha/\alpha_0$) (at design temperature)
T10A42	IG110	MB	AX	750	692	13.4	-16.3%
T10A43	IG110	MB	AX	750	692	13.4	-13.0%
T10A45	IG110	MB	AX	750	675	27.2	-40.3%
T10A46	IG110	MB	AX	750	675	27.2	-32.9%
T10A44	IG110	MB	AX	750	675	27.2	-32.1%
T10A49	IG110	MB	AX	750	607	31.8	-47.2%
T10A51	IG110	MB	AX	750	607	31.8	-52.6%
T10A53	IG110	MB	AX	750	634	31.8	-53.2%
T10T41	IG110	MB	TR	750	664	13.4	-19.9%
T10T42	IG110	MB	TR	750	692	13.4	-14.5%
T10T43	IG110	MB	TR	750	692	13.4	-15.2%
T10T45	IG110	MB	TR	750	675	27.2	-37.0%
T10T46	IG110	MB	TR	750	675	27.2	-36.2%
T10T47	IG110	MB	TR	750	682	27.2	-39.1%
T10T49	IG110	MB	TR	750	607	31.8	-33.9%
T10T50	IG110	MB	TR	750	607	31.8	-59.0%
T10T51	IG110	MB	TR	750	607	31.8	-46.9%

B.3 POST-IRRADIATION FLEXURAL STRENGTH

ID	Material	Sample Type	Orien.	Design Temp. (°C)	Measured Temp. (°C)	Neutron Fluence ($x10^{25}$ n/m^2 [E>0.1 MeV])	Flexural Strength Change ($\Delta\sigma/\sigma_0$)
T10A00	IG110	MB	AX	300	347	13.4	1.16
T10A01	IG110	MB	AX	300	347	13.4	1.04
T10A02	IG110	MB	AX	300	347	13.4	1.06
T10A03	IG110	MB	AX	300	291	13.4	0.90
T10A04	IG110	MB	AX	300	291	13.4	1.00
T10A05	IG110	MB	AX	300	410	25.3	1.18
T10A06	IG110	MB	AX	300	410	25.3	1.24
T10A07	IG110	MB	AX	300	410	25.3	0.74
T10A08	IG110	MB	AX	300	426	25.3	0.97
T10A09	IG110	MB	AX	300	426	25.3	1.13
T10A10	IG110	MB	AX	300	405	37.0	0.57
T10A11	IG110	MB	AX	300	405	37.0	0.90
T10A13	IG110	MB	AX	300	393	37.0	1.12
T10A14	IG110	MB	AX	300	393	37.0	0.64
T10T00	IG110	MB	TR	300	347	13.4	1.23
T10T01	IG110	MB	TR	300	347	13.4	1.11
T10T02	IG110	MB	TR	300	347	13.4	1.09
T10T03	IG110	MB	TR	300	291	13.4	1.05
T10T69	IG110	MB	TR	300	291	13.4	1.20
T10T05	IG110	MB	TR	300	410	25.3	1.17
T10T06	IG110	MB	TR	300	410	25.3	1.36
T10T07	IG110	MB	TR	300	410	25.3	1.04
T10T08	IG110	MB	TR	300	426	25.3	1.06
T10T09	IG110	MB	TR	300	426	25.3	1.24
T10T10	IG110	MB	TR	300	405	37.0	0.94
T10T11	IG110	MB	TR	300	405	37.0	0.81
T10T12	IG110	MB	TR	300	405	37.0	0.75
T10T13	IG110	MB	TR	300	393	37.0	1.02
T10T14	IG110	MB	TR	300	393	37.0	0.87
T10A15	IG110	MB	AX	450	459	14.3	0.75
T10A16	IG110	MB	AX	450	459	14.3	0.99
T10A17	IG110	MB	AX	450	459	14.3	0.80
T10A18	IG110	MB	AX	450	493	14.3	0.87
T10A19	IG110	MB	AX	450	493	14.3	0.85
T10A20	IG110	MB	AX	450	482	27.0	1.05
T10A21	IG110	MB	AX	450	482	27.0	0.66
T10A22	IG110	MB	AX	450	482	27.0	0.93
T10A23	IG110	MB	AX	450	383	27.0	0.87
T10A28	IG110	MB	AX	450	495	37.5	0.31
T10T15	IG110	MB	TR	450	459	14.3	0.91
T10T16	IG110	MB	TR	450	459	14.3	0.88
T10T17	IG110	MB	TR	450	459	14.3	0.92
T10T18	IG110	MB	TR	450	493	14.3	0.93
T10T19	IG110	MB	TR	450	493	14.3	0.81
T10T20	IG110	MB	TR	450	482	27.0	1.06
T10T21	IG110	MB	TR	450	482	27.0	0.94
T10T22	IG110	MB	TR	450	482	27.0	0.99
T10T23	IG110	MB	TR	450	383	27.0	1.03
T10T24	IG110	MB	TR	450	383	27.0	1.06
T10T26	IG110	MB	TR	450	517	37.4	0.49
T10T27	IG110	MB	TR	450	517	37.4	0.43
T10T28	IG110	MB	TR	450	495	37.5	0.40
T10A30	IG110	MB	AX	600	667	14.3	0.81
T10A31	IG110	MB	AX	600	667	14.3	0.73
T10A32	IG110	MB	AX	600	667	14.3	0.70

ID	Material	Sample Type	Orien.	Design Temp. (°C)	Measured Temp. (°C)	Neutron Fluence ($x10^{25}$ n/m^2 [E>0.1 MeV])	Flexural Strength Change ($\Delta\sigma/\sigma_0$)
T10A33	IG110	MB	AX	600	662	27.0	0.54
T10A34	IG110	MB	AX	600	662	27.0	0.82
T10A35	IG110	MB	AX	600	662	27.0	0.61
T10A36	IG110	MB	AX	600	588	37.4	-0.03
T10T30	IG110	MB	TR	600	667	14.3	0.97
T10T31	IG110	MB	TR	600	667	14.3	0.86
T10T32	IG110	MB	TR	600	667	14.3	0.90
T10T33	IG110	MB	TR	600	662	27.0	0.95
T10T34	IG110	MB	TR	600	662	27.0	0.72
T10T35	IG110	MB	TR	600	662	27.0	0.62
T10T38	IG110	MB	TR	600	588	37.4	0.16
T10A39	IG110	MB	AX	750	664	13.4	1.00
T10A40	IG110	MB	AX	750	664	13.4	0.88
T10A41	IG110	MB	AX	750	664	13.4	0.94
T10A42	IG110	MB	AX	750	692	13.4	0.66
T10A43	IG110	MB	AX	750	692	13.4	0.71
T10A45	IG110	MB	AX	750	675	27.2	0.64
T10A46	IG110	MB	AX	750	675	27.2	0.70
T10A47	IG110	MB	AX	750	682	27.2	0.31
T10A48	IG110	MB	AX	750	682	27.2	0.29
T10A50	IG110	MB	AX	750	607	31.8	0.20
T10A52	IG110	MB	AX	750	634	31.8	0.65
T10T39	IG110	MB	TR	750	664	13.4	0.83
T10T40	IG110	MB	TR	750	664	13.4	0.83
T10T41	IG110	MB	TR	750	664	13.4	0.71
T10T42	IG110	MB	TR	750	692	13.4	0.55
T10T43	IG110	MB	TR	750	692	13.4	0.90
T10T45	IG110	MB	TR	750	675	27.2	0.40
T10T46	IG110	MB	TR	750	675	27.2	0.40
T10T47	IG110	MB	TR	750	682	27.2	0.45
T10T48	IG110	MB	TR	750	682	27.2	0.31
T10T52	IG110	MB	TR	750	634	31.8	0.06

B.4 POST-IRRADIATION COMPRESSION STRENGTH

ID	Material	Sample Type	Orien.	Design Temp. (°C)	Measured Temp. (°C)	Neutron Fluence ($x10^{25}$ n/m^2 [E>0.1 MeV])	Compression Strength Change ($\Delta\sigma/\sigma_0$)
T14A40	IG110	CRP	AX	300	238	12.2	1.07
T14A39	IG110	CRP	AX	300	239	12.6	1.33
T13A34	IG110	CRS	AX	300	245	13.0	1.21
T14A55	IG110	CRP	AX	300	240	21.7	0.65
T14A54	IG110	CRP	AX	300	241	22.4	1.63
T13A67	IG110	CRS	AX	300	248	23.1	0.96
T14A63	IG110	CRP	AX	300	256	32.3	0.76
T14A64	IG110	CRP	AX	300	257	33.4	0.84
T13A28	IG110	CRS	AX	300	264	34.4	0.73
T14A41	IG110	CRP	AX	450	389	14.7	0.20
T14A42	IG110	CRP	AX	450	388	14.9	0.26
T13A35	IG110	CRS	AX	450	399	15.2	0.61
T14A56	IG110	CRP	AX	450	367	26.2	0.33
T14A57	IG110	CRP	AX	450	367	26.6	0.22
T13A23	IG110	CRS	AX	450	377	27.0	0.71
T14A65	IG110	CRP	AX	450	385	38.9	0.50
T14A66	IG110	CRP	AX	450	384	39.5	0.44
T13A29	IG110	CRS	AX	450	395	40.1	0.14
T14A44	IG110	CRP	AX	600	488	16.0	0.33
T14A43	IG110	CRP	AX	600	489	16.1	0.33
T13A36	IG110	CRS	AX	600	487	16.1	0.29
T14A58	IG110	CRP	AX	600	508	28.5	0.28
T14A59	IG110	CRP	AX	600	509	28.6	0.42
T13A24	IG110	CRS	AX	600	506	28.7	0.41
T14A67	IG110	CRP	AX	600	478	42.3	-0.43
T14A68	IG110	CRP	AX	600	479	42.6	-0.06
T13A30	IG110	CRS	AX	600	477	42.7	-0.20
T13A04	IG110	CRS	AX	750	700	13.4	1.00
T13A05	IG110	CRS	AX	750	700	13.4	0.66
T13A06	IG110	CRS	AX	750	700	13.4	1.11
T13A07	IG110	CRS	AX	750	642	27.2	-0.01
T13A08	IG110	CRS	AX	750	642	27.2	0.05
T13A09	IG110	CRS	AX	750	642	27.2	0.25
T13A10	IG110	CRS	AX	750	637	31.8	0.06
T13A11	IG110	CRS	AX	750	637	31.8	0.01
T13A12	IG110	CRS	AX	750	637	31.8	0.33

B.5 POST-IRRADIATION THERMAL CONDUCTIVITY

B.5.1 Room Temperature

ID	Material	Sample Type	Orien.	Design Temp. (°C)	Measured Temp. (°C)	Neutron Fluence ($x10^{25}$ n/m^2 [E>0.1 MeV])	Thermal Conductivity @25°C (W/m/K)
T11T34	IG110	TD3	TR	300	238	11.4	2.36
T11T33	IG110	TD3	TR	300	238	11.6	2.32
T11T32	IG110	TD3	TR	300	238	11.8	2.36
T11T31	IG110	TD3	TR	300	238	11.9	2.41
T11T30	IG110	TD3	TR	300	238	12.1	2.28
T11T04	IG110	TD3	TR	300	240	20.3	3.65
T11T03	IG110	TD3	TR	300	240	20.6	3.57
T11T02	IG110	TD3	TR	300	240	20.9	3.61
T11T01	IG110	TD3	TR	300	240	21.2	3.70
T11T00	IG110	TD3	TR	300	240	21.5	3.59
T11T19	IG110	TD3	TR	300	256	30.2	2.60
T11T18	IG110	TD3	TR	300	256	30.7	2.72
T11T17	IG110	TD3	TR	300	256	31.1	2.71
T11T16	IG110	TD3	TR	300	256	31.5	2.72
T11T15	IG110	TD3	TR	300	256	31.9	2.80
T11T39	IG110	TD3	TR	450	380	14.2	13.15
T11T38	IG110	TD3	TR	450	385	14.3	12.80
T11T37	IG110	TD3	TR	450	388	14.4	12.85
T11T36	IG110	TD3	TR	450	389	14.5	12.61
T11T35	IG110	TD3	TR	450	389	14.6	12.62
T11T09	IG110	TD3	TR	450	359	25.3	17.61
T11T08	IG110	TD3	TR	450	364	25.5	17.41
T11T07	IG110	TD3	TR	450	366	25.6	18.15
T11T06	IG110	TD3	TR	450	367	25.8	16.98
T11T05	IG110	TD3	TR	450	367	26.0	18.32
T11T24	IG110	TD3	TR	450	377	37.6	10.97
T11T23	IG110	TD3	TR	450	381	37.9	10.89
T11T22	IG110	TD3	TR	450	384	38.1	9.94
T11T21	IG110	TD3	TR	450	385	38.4	9.72
T11T20	IG110	TD3	TR	450	385	38.7	9.54
T11T44	IG110	TD3	TR	600	483	15.8	18.25
T11T43	IG110	TD3	TR	600	485	15.8	18.67
T11T42	IG110	TD3	TR	600	486	15.9	18.94
T11T41	IG110	TD3	TR	600	487	15.9	18.69
T11T40	IG110	TD3	TR	600	487	16.0	18.61
T11T13	IG110	TD3	TR	600	502	28.1	23.01
T11T12	Lost during disassembly						
T11T11	IG110	TD3	TR	600	506	28.3	21.98
T11T10	IG110	TD3	TR	600	506	28.3	22.01
T11T14	IG110	TD3	TR	600	507	28.4	21.95
T11T29	IG110	TD3	TR	600	473	41.8	10.18
T11T28	IG110	TD3	TR	600	475	41.9	10.23
T11T27	IG110	TD3	TR	600	476	42.0	10.30
T11T26	IG110	TD3	TR	600	476	42.1	8.94
T11T25	IG110	TD3	TR	600	477	42.2	10.32
T12T00	IG110	TD4	TR	750	700	13.4	22.27
T12T01	IG110	TD4	TR	750	700	13.4	22.28
T12T02	IG110	TD4	TR	750	700	13.4	25.90
T12T03	IG110	TD4	TR	750	700	13.4	26.19
T12T04	IG110	TD4	TR	750	700	13.4	22.44
T12T05	IG110	TD4	TR	750	642	27.2	11.16
T12T06	IG110	TD4	TR	750	642	27.2	10.35
T12T07	IG110	TD4	TR	750	642	27.2	10.44

ID	Material	Sample Type	Orien.	Design Temp. (°C)	Measured Temp. (°C)	Neutron Fluence ($x10^{25}$ n/m^2 [E>0.1 MeV])	Thermal Conductivity @25°C (W/m/K)
T12T08	IG110	TD4	TR	750	642	27.2	11.17
T12T09	IG110	TD4	TR	750	642	27.2	11.39
T12T10	IG110	TD4	TR	750	637	31.8	7.48
T12T11	IG110	TD4	TR	750	637	31.8	7.43
T12T12	IG110	TD4	TR	750	637	31.8	7.05
T12T13	IG110	TD4	TR	750	637	31.8	8.34
T12T14	IG110	TD4	TR	750	637	31.8	9.10

B.5.2 Designed Irradiation Temperature

ID	Material	Sample Type	Orien.	Design Temp. (°C)	Measured Temp. (°C)	Neutron Fluence ($x10^{25}$ n/m^2 [E>0.1 MeV])	Thermal Conductivity Change ($\Delta K/K_0$)
T11T34	IG110	TD3	TR	300	238	11.4	-0.97
T11T33	IG110	TD3	TR	300	238	11.6	-0.97
T11T32	IG110	TD3	TR	300	238	11.8	-0.97
T11T31	IG110	TD3	TR	300	238	11.9	-0.97
T11T30	IG110	TD3	TR	300	238	12.1	-0.97
T11T04	IG110	TD3	TR	300	240	20.3	-0.95
T11T03	IG110	TD3	TR	300	240	20.6	-0.95
T11T02	IG110	TD3	TR	300	240	20.9	-0.95
T11T01	IG110	TD3	TR	300	240	21.2	-0.95
T11T00	IG110	TD3	TR	300	240	21.5	-0.95
T11T19	IG110	TD3	TR	300	256	30.2	-0.96
T11T18	IG110	TD3	TR	300	256	30.7	-0.96
T11T17	IG110	TD3	TR	300	256	31.1	-0.96
T11T16	IG110	TD3	TR	300	256	31.5	-0.96
T11T15	IG110	TD3	TR	300	256	31.9	-0.96
T11T39	IG110	TD3	TR	450	380	14.2	-0.80
T11T38	IG110	TD3	TR	450	385	14.3	-0.80
T11T37	IG110	TD3	TR	450	388	14.4	-0.80
T11T36	IG110	TD3	TR	450	389	14.5	-0.80
T11T35	IG110	TD3	TR	450	389	14.6	-0.80
T11T09	IG110	TD3	TR	450	359	25.3	-0.71
T11T08	IG110	TD3	TR	450	364	25.5	-0.72
T11T07	IG110	TD3	TR	450	366	25.6	-0.71
T11T06	IG110	TD3	TR	450	367	25.8	-0.73
T11T05	IG110	TD3	TR	450	367	26.0	-0.70
T11T24	IG110	TD3	TR	450	377	37.6	-0.82
T11T23	IG110	TD3	TR	450	381	37.9	-0.82
T11T22	IG110	TD3	TR	450	384	38.1	-0.84
T11T21	IG110	TD3	TR	450	385	38.4	-0.84
T11T20	IG110	TD3	TR	450	385	38.7	-0.84
T11T44	IG110	TD3	TR	600	483	15.8	-0.67
T11T43	IG110	TD3	TR	600	485	15.8	-0.66
T11T42	IG110	TD3	TR	600	486	15.9	-0.66
T11T41	IG110	TD3	TR	600	487	15.9	-0.66
T11T40	IG110	TD3	TR	600	487	16.0	-0.66
T11T13	IG110	TD3	TR	600	502	28.1	-0.57
T11T12	Lost during disassembly						
T11T11	IG110	TD3	TR	600	506	28.3	-0.58
T11T10	IG110	TD3	TR	600	506	28.3	-0.59
T11T14	IG110	TD3	TR	600	507	28.4	-0.59
T11T29	IG110	TD3	TR	600	473	41.8	-0.80
T11T28	IG110	TD3	TR	600	475	41.9	-0.80
T11T27	IG110	TD3	TR	600	476	42.0	-0.80
T11T26	IG110	TD3	TR	600	476	42.1	-0.83
T11T25	IG110	TD3	TR	600	477	42.2	-0.80
T12T00	IG110	TD4	TR	750	700	13.4	-0.55
T12T01	IG110	TD4	TR	750	700	13.4	-0.55
T12T02	IG110	TD4	TR	750	700	13.4	-0.55
T12T03	IG110	TD4	TR	750	700	13.4	-0.54
T12T04	IG110	TD4	TR	750	700	13.4	-0.55
T12T05	IG110	TD4	TR	750	642	27.2	-0.75
T12T06	IG110	TD4	TR	750	642	27.2	-0.77
T12T07	IG110	TD4	TR	750	642	27.2	-0.76
T12T08	IG110	TD4	TR	750	642	27.2	-0.75
T12T09	IG110	TD4	TR	750	642	27.2	-0.75

ID	Material	Sample Type	Orien.	Design Temp. (°C)	Measured Temp. (°C)	Neutron Fluence ($x10^{25}$ n/m^2 [E>0.1 MeV])	Thermal Conductivity Change ($\Delta K/K_0$)
T12T10	IG110	TD4	TR	750	637	31.8	-0.83
T12T11	IG110	TD4	TR	750	637	31.8	-0.83
T12T12	IG110	TD4	TR	750	637	31.8	-0.84
T12T13	IG110	TD4	TR	750	637	31.8	-0.80
T12T14	IG110	TD4	TR	750	637	31.8	-0.79

B.6 IRRADIATION CREEP

ID	Material	Sample Type	Orien.	Creep	Design Temp. (°C)	Measured Temp. (°C)	Neutron Fluence ($x10^{25}$ n/m^2 [E>0.1 MeV])	Length Change ($\Delta L/L_0$)
T14A38	IG110	CRP	AX	Stressed	300	243	10.8	-3.07%
T14A37	IG110	CRP	AX	Stressed	300	243	11.2	-3.02%
T13A33	IG110	CRS	AX	Stressed	300	243	11.8	-3.33%
T14A36	IG110	CRP	AX	Stressed	300	244	12.3	-3.35%
T14A35	IG110	CRP	AX	Stressed	300	253	12.8	-3.43%
T14A50	Lost during disassembly							
T14A49	IG110	CRP	AX	Stressed	300	226	19.9	-3.64%
T13A21	IG110	CRS	AX	Stressed	300	226	20.9	-3.76%
T14A48	IG110	CRP	AX	Stressed	300	227	21.9	-2.81%
T14A47	IG110	CRP	AX	Stressed	300	235	22.8	-3.43%
T14A74	IG110	CRP	AX	Stressed	300	240	28.6	-4.09%
T14A73	IG110	CRP	AX	Stressed	300	241	29.6	-3.77%
T13A27	IG110	CRS	AX	Stressed	300	241	31.1	-4.36%
T14A62	IG110	CRP	AX	Stressed	300	242	32.5	-4.45%
T14A34	IG110	CRP	AX	Stressed	300	251	33.9	-5.87%
T14A40	IG110	CRP	AX	Unstressed	300	238	12.2	1.28%
T14A39	IG110	CRP	AX	Unstressed	300	239	12.6	1.69%
T13A34	IG110	CRS	AX	Unstressed	300	245	13.0	1.05%
T14A55	IG110	CRP	AX	Unstressed	300	240	21.7	1.39%
T14A54	IG110	CRP	AX	Unstressed	300	241	22.4	1.43%
T13A67	IG110	CRS	AX	Unstressed	300	248	23.1	0.47%
T14A63	IG110	CRP	AX	Unstressed	300	256	32.3	2.52%
T14A64	IG110	CRP	AX	Unstressed	300	257	33.4	2.57%
T13A28	IG110	CRS	AX	Unstressed	300	264	34.4	1.93%
T14A72	IG110	CRP	AX	Stressed	600	496	15.6	-3.43%
T14A71	IG110	CRP	AX	Stressed	600	500	15.8	-3.42%
T13A31	IG110	CRS	AX	Stressed	600	501	15.9	-3.31%
T14A70	IG110	CRP	AX	Stressed	600	502	16.1	-3.59%
T14A69	IG110	CRP	AX	Stressed	600	505	16.1	-3.30%
T14A45	IG110	CRP	AX	Stressed	600	515	27.7	-2.48%
T14A02	Lost during disassembly							
T13A19	IG110	CRS	AX	Stressed	600	521	28.3	-1.58%
T14A01	IG110	CRP	AX	Stressed	600	522	28.6	-2.22%
T14A00	IG110	CRP	AX	Stressed	600	524	28.7	-2.24%
T14A60	IG110	CRP	AX	Stressed	600	481	41.2	-0.15%
T14A53	IG110	CRP	AX	Stressed	600	485	41.8	-0.64%
T13A25	IG110	CRS	AX	Stressed	600	486	42.2	-0.85%
T14A52	IG110	CRP	AX	Stressed	600	487	42.5	0.26%
T14A51	IG110	CRP	AX	Stressed	600	489	42.7	-0.09%
T14A44	IG110	CRP	AX	Unstressed	600	488	16.0	-1.84%
T14A43	IG110	CRP	AX	Unstressed	600	489	16.1	-1.82%
T13A36	IG110	CRS	AX	Unstressed	600	487	16.1	-1.91%
T14A58	IG110	CRP	AX	Unstressed	600	508	28.5	0.28%
T14A59	IG110	CRP	AX	Unstressed	600	509	28.6	-0.13%
T13A24	IG110	CRS	AX	Unstressed	600	506	28.7	-1.07%
T14A67	IG110	CRP	AX	Unstressed	600	478	42.3	3.67%
T14A68	IG110	CRP	AX	Unstressed	600	479	42.6	4.17%
T13A30	IG110	CRS	AX	Unstressed	600	477	42.7	4.39%

INTERNAL DISTRIBUTION

1. Y. Katoh
2. A.A. Campbell
3. K.D. Linton
4. T.D. Burchell
5. M. Vance

EXTERNAL DISTRIBUTION

6. Mr. Masatoshi Yamaji, Toyo Tanso Co., Ltd., Telephone +81-875-83-6917, email: myamaji@toyotanso.co.jp
7. Mr. Eiji Kunimoto, Toyo Tanso Co., Ltd., Telephone +81-875-83-6917, email: e.kunimoto@toyotanso.co.jp
8. Mr. Thomas J. O'Connor, DOE Office of Nuclear Energy, NE-20/GTN, Telephone: (301) 903-6781, email: Tom.Oconnor@hq.doe.gov